



TECHNISCHE
UNIVERSITÄT
WIEN

VIENNA
UNIVERSITY OF
TECHNOLOGY

Diplomarbeit

Magnetization Dynamics and Thermal Stability of Spin-Chains

Ausgeführt am Institut für Festkörperphysik
der Technischen Universität Wien
unter der Anleitung von

Privatdoz. Dipl.-Ing. Dr. techn. Dieter Suess

durch

Roman Pechhacker

Matrikelnummer: 0126151

Musnergasse 13

A-1220 Wien

Wien, am February 25, 2010

Abstract

The objective of the diploma thesis is to demonstrate dynamics of magnetic systems based on the theory of micromagnetics and find an analytical approach to calculate Ω_0 for spin-chains. After a basic introduction on thermodynamics, that involves the formulation of an effective magnetic field and stresses its important contributions (e.g. Zeeman-, anisotropy- and exchange-terms), requirements for the minimization of Gibbs Free Energy are given. In chapter 3 the dynamics of single- and multi-particle magnetic systems is analyzed using the Landau-Lifshitz-Gilbert Equation. A finite difference scheme is used to solve the Landau-Lifshitz-Gilbert equation numerically for a magnetic spin-chain. At first the relaxation of a magnetic system into its energetic minimum is simulated. Then magnetization reversal processes as a result of externally applied magnetic fields are investigated. In chapter 4 magnetization reversals due to thermal activity are described by use of the Arrhenius-Néel Equation, which features the attempt frequency. In the following the attempt frequency is given as a product of a dynamic factor λ_+ and a statistical prefactor Ω_0 , as stated by Braun [Bra94]. Furthermore the required Hessians for the calculation of Ω_0 are derived and an analytical solution for the single-spin-system is given. The analytical derivation of the multi-spin-system is given and simulations are carried out, varying total system size and number of spins. The simulations show that the results depend on the total system size. It could be shown, that cell size of the finite difference discretization does not change the results of Ω_0 . Additionally eigenfunctions of the Hessian are analyzed with respect to a Fourier mode representation of the Gibbs Free Energy and magnetization as suggested in [Md09]. Finally the ratio of the eigenvalues of the Hessians for minimum- and saddle-point-configurations are plotted and fitted by an exponential function. The plot shows that not all ratios of eigenvalues need to be taken into account in order to calculate a sufficiently accurate value of Ω_0 .

Contents

1	Introduction	5
2	Basics of Micromagnetism	7
2.1	Maxwell's Equations	7
2.2	Thermodynamic Description of Magnetic Systems	7
2.2.1	Gibb's Free Energy	7
2.2.2	Zeeman Term	8
2.2.3	Exchange Interaction	9
2.2.4	Magnetocrystalline Anisotropy	10
2.2.5	Omitted Terms	11
2.3	Minimization of the Gibb's Free Energy	11
2.4	Finite Difference Method	12
3	Dynamical Analysis of Micromagnetics	14
3.1	Landau Lifschitz Gilbert Equation	14
3.2	Solid Body Systems	16
3.2.1	Single Spin System	16
3.2.2	3 Spin System	18
3.3	Magnetization Alteration Analysis	20
3.3.1	40 Spin System	21
3.3.2	2×40 Spin System	22
3.3.3	Conclusion	23
4	Analytical Calculation of the Attempt Frequency	27
4.1	Thoughts on Stability	27
4.2	Attempt Frequency	28
4.3	The Statistical Prefactor Ω_0	28
4.4	Spherical Hessian	29

Contents

4.5	Single Spin System	31
4.5.1	Single Spin Spherical Hessian	31
4.5.2	Minimum and Saddle-Point Configurations	33
4.5.3	Explicit Calculation	34
4.6	Multi-Spin Problem	35
4.6.1	Multi-Spin Spherical Hessian	35
4.6.2	Explicit Calculations	37
4.7	Eigenvectors and Eigenfunctions	37
4.8	Eigenvalue Analysis	42
5	Conclusion and Outlook	49
6	Bibliography	50

1 Introduction

Magnetic structures on the scale of nanometers have seen much development in recent years. Fields of application reach from data storage devices to applied biology. The magnetization states of such systems are subject to stability questions. Typically there are two reasons for the change of a certain magnetization state. Firstly - and obviously - magnetization configurations can be affected by application of external magnetic fields. Most prominent are of course hysteresis curves that result from such experiments. Such a change of configuration is mostly intended, since it basically describes a writing or measuring process. Secondly, thermal activation can result in loss of a set configuration. In case of data storage, such a loss is usually unintended and equivalent to the loss of information (i.e. data).

Experimental research on this field proves somewhat difficult, because data storage media should be able to work for a very long period of time (i.e. many years). Intuitively, it is not a very efficient method to keep testing recording media for 10 to 20 years in order to prove their technical capability. Therefore computer simulations are a predominant line of research in this field, if it is possible to find a theoretical foundation, on which to build a formalism, that allows to analyze magnetization behavior as a function of time. Such simulations can speed up investigations and promise much more efficient research in this field.

The objective of this work is a basic description of magnetization dynamics with special stress upon magnetization switching as a reaction to an applied magnetic field. In order to find a suitable theory for such a system the theory of micromagnetism, as was first presented by W.F. Brown in the 1960s [Bro63b], is applied. Within this semi-classical environment the Landau-Lifschitz-Gilbert Equation describes magnetization dynamics for various damping limits.

Furthermore sudden magnetization switching due to thermal activation is discussed by use of the Arrhenius-Néel law. It describes the lifetime of a magnetic state by means of a temperature-independent attempt frequency. Temperature is taken into account by an exponential term that is the ratio of energy barrier over temperature. The energy barrier separates the two magnetic stable states. Most attention is directed onto the attempt frequency, which can be expressed by a statistical factor Ω_0 and a dynamical one λ_+ . The dynamical factor results from the

1 Introduction

Landau-Lifschitz-Gilbert Equation and therefore is highly dependent on the damping, giving rise to two main lines of research VDL (very low damping limit) and IDL (intermediate to high damping limit). The statistical factor results from second derivatives of the Gibb's Free Energy with respect to the set of spherical coordinates under the boundary condition of $r = \text{constant}$. A formalism will be derived that points out single particle calculations of Ω_0 and extend it to the multi-particle problem, providing an analytical approach to calculate the statistical factor, that offers eradication of numerical derivation of the Hessian.

2 Basics of Micromagnetism

2.1 Maxwell's Equations

The phenomenon of electromagnetism was discovered in the 19th century. The most profound theoretical description is given by the set of Maxwell's equations

$$\begin{aligned}\nabla \mathbf{D} &= \rho & \nabla \times \mathbf{E} &= -\frac{\partial \mathbf{B}}{\partial t} \\ \nabla \mathbf{B} &= 0 & \nabla \times \mathbf{H} &= \mathbf{j} + \frac{\partial \mathbf{D}}{\partial t}\end{aligned}\tag{2.1}$$

2.2 Thermodynamic Description of Magnetic Systems

2.2.1 Gibb's Free Energy

Magnetic systems are described by the so-called Gibb's Free Energy. To derive it we start at the Inner Energy $U(S, M, N)$, which is a function of extensive variables entropy S , magnetization M , and mole number N ; as well as their conjugate intensive variables temperature T , magnetic field H_m , and chemical potential μ [GB06]. Any change of Inner Energy can be given by

$$dU = TdS + \mu_0 H_m dM + \mu dN\tag{2.2}$$

where μ_0 is the magnetic permeability.

In our case, we will consider systems for which particle transfer with the environment is prohibited, making $dN = 0$. The entropy S and the magnetization M remain state defining

variables. Performing a Legendre transformation we define the enthalpy H

$$\begin{aligned} H(T, M) &= U - TS \\ dH &= dU - TdS - SdT \end{aligned} \quad (2.3)$$

Performing a second transformation we arrive at Gibb's Free Energy E .

$$\begin{aligned} E(T, H) &= H - \mu_0 M H_m \\ dE &= dH - \mu_0 M dH_m - \mu_0 H_m dM \\ dE &= dU - TdS - SdT - \mu_0 M dH_m - \mu_0 H_m dM \end{aligned} \quad (2.4)$$

Since all fields that result from sources within the system are already accounted for by the Inner Energy U , the field H_m in 2.4 has to be external. In the following we will assume that H_{ext} remains constant for longer than the relaxation time of the magnetic system, canceling the term $dH_{ext} = 0$. If we furthermore consider isothermal ($dT = 0$) processes we can further simplify the expression, and by choosing $T = 0$ we arrive at

$$dE(T, M) = dU - \mu_0 H_{ext} dM \quad (2.5)$$

2.5 consists of two main terms, the first is the Inner Energy of the system, mainly consisting of the exchange interaction, the magnetocrystalline anisotropy and scattering energy, the second is the Zeeman Energy. In the following we will outline these important contributions to E .

2.2.2 Zeeman Term

The Zeeman energy E_Z describes the change of a systems energy due to application of an external magnetic field. In micromagnetics we use the term to account for the magnetization distribution \mathbf{M} interacting with externally applied fields. We define the Zeeman term as

$$E_Z = -\mu_0 \int \mathbf{H}_{ext} \cdot \mathbf{M} dV \quad (2.6)$$

We see that E_Z is minimized for parallel alignment of external field \mathbf{H}_{ext} and magnetization \mathbf{M} . Such a state would be energetically favorable because of the minus sign in 2.6.

2.2.3 Exchange Interaction

The dominant contribution to the Inner Energy U originates from the interaction between the magnetic moments. Within a quantum mechanic formalism, spins of a ferromagnet tend to line up parallel to each other, whereas in antiferromagnets they tend to align antiparallel. The most principle way of treating this behavior is by means of the Heisenberg Hamiltonian [Aha96]

$$\mathcal{H} = - \sum_{i \neq j} J_{i,j} \mathbf{S}_i \cdot \mathbf{S}_j \quad (2.7)$$

with $J_{i,j}$ being the exchange integral

$$J_{i,j} = 2 \int \phi_i^*(\mathbf{r}_1) \phi_j^*(\mathbf{r}_2) \frac{e^2}{|\mathbf{r}_1 - \mathbf{r}_2|} \phi_i(\mathbf{r}_1) \phi_j(\mathbf{r}_2) d\mathbf{r}_1 d\mathbf{r}_2 \quad (2.8)$$

where $\phi_i(\mathbf{r}_j)$ are wavefunctions of a spin carrier (e.g. an electron), containing information on both spatial distribution and spin, given at the site \mathbf{r}_j , and e is the elementary electric charge. The integral features the overlap of those wavefunctions. For ferromagnetic systems J is positive $J_{ferro} > 0$, while for antiferromagnets it is negative $J_{anti} < 0$. Since overlaps decrease quickly, the further the spins are away from each other, it is sufficient for most calculations, to take only next neighbor interaction into account. We therefore rewrite 2.9 as

$$\mathcal{H} = -J \sum_{NN} \mathbf{S}_i \cdot \mathbf{S}_j \quad (2.9)$$

With η_{ij} being the angle between \mathbf{S}_i and \mathbf{S}_j , we (Taylor-)expand the cosine function, redefine the zero level of the exchange energy, and use

$$|\eta_{ij}| \approx \frac{1}{M_s} |\mathbf{M}_i - \mathbf{M}_j| \approx |(\mathbf{r}_i \cdot \nabla) \frac{\mathbf{M}}{M_s}|$$

Inserting this into 2.9 and changing the sum into an integral over the system, yields under the usage of $\mathbf{u} = \frac{\mathbf{M}}{M_s}$

$$E_{xch} = A \int [(\nabla u_x)^2 + (\nabla u_y)^2 + (\nabla u_z)^2] dV \quad (2.10)$$

with the exchange constant

$$A = \frac{JS^2}{a} \rho$$

where a is the distance between neighboring spins and ρ is a parameter that depends on the number of nearest neighbors, which is defined by the crystal structure [Sch06].

2.2.4 Magnetocrystalline Anisotropy

A hysteresis curve depicts the fact that magnetization is not a sole result of externally applied fields. It can be evoked by them, but once the field is switched off again, the magnetization does not necessarily decay to zero as well. In absence of an external field this effect can not be explained by the Zeeman term 2.6, nor does the exchange interaction give a satisfying answer. The exchange interaction in a ferromagnet tries to align spins parallel to one another. Since the Heisenberg Hamiltonian is isotropic no specific direction in space is favored by the exchange energy. Within a real solid state ferromagnetic body there are directions, which are preferable for the magnetization \mathbf{M} to point into. They result from the spin-orbit interaction of the electrons. The orbits are depending on the crystallographic structure and the interaction makes spins align along certain axes within the crystal [Aha96].

These axes need not be the same throughout the magnet, nor is their number forcefully the same everywhere. It is not unusual, that in some regions of a solid body, magnetization is oriented in a different direction compared to others. Those domains were first interpreted by Weiss and he gave them his name.

Effectively, anisotropy makes it easier to align spins along certain directions in space within a solid state body. This is a very important property concerning data storage. To enable data storage on magnetic media it is essential that magnetization distributions are stable for a macroscopic period of time after it has been established; e.g. by application of an external magnetic field. The anisotropy gives rise to the idea that no additional power source is needed

to maintain a magnetic state. This notion is, however, subject to stability considerations and will be coped with later.

A fundamental derivation of the anisotropy energy is hardly ever needed [Aha96] and we introduce a phenomenological approach. In the following we will concentrate on uniaxial anisotropy. The direction which is preferable to the spins will be called 'easy'-direction.

Let θ be the angle between the 'easy'-direction's unit vector \mathbf{k} and the magnetization unit vector $\mathbf{u} = \frac{\mathbf{M}}{M_s}$, then

$$\begin{aligned} E_{ani} &= VK_1 \left(1 - (\mathbf{u} \cdot \mathbf{k})^2\right) + VK_2 (\mathbf{u} \cdot \mathbf{k})^4 + \dots \\ &= VK_1 (1 - \cos^2 \theta) + VK_2 \cos^4 \theta + \dots \end{aligned} \quad (2.11)$$

with M_s being the saturation magnetization. Experiments show that uniaxial anisotropy is symmetric with respect to the plane perpendicular to the 'easy'-direction, hence we can safely omit all odd powers of $\mathbf{u} \cdot \mathbf{k}$. For most applications we can neglect all terms except the first featuring K_1 , which will be the case for all calculations within this work.

2.2.5 Omitted Terms

A full description of the Inner Energy should also contain contributions from surface anisotropies and a demagnetizing term, which can be derived from the Maxwell Equations 2.1. The stray-field and the surface anisotropy of a magnetic spin chain, can be approximated by an additional contribution to the uniaxial anisotropy.

2.3 Minimization of the Gibb's Free Energy

A magnetization state of equilibrium must mean that the Gibb's Free Energy E is at a minimum. Later we will study minimum configurations, therefore we will take a look at how a magnetization configuration can be found, that minimizes E .

Since the Gibb's Free Energy is a functional of the magnetization distribution \mathbf{M} , it takes a functional derivative to find a minimum. Brown solved the problem by introducing a variational method, examining how E reacted to small variations of \mathbf{M} under the boundary condition that $|\mathbf{M}| = M_s = \text{const.}$

$$\frac{1}{\mu_0} \frac{\delta E}{\delta \mathbf{M}} = 0 \quad (2.12)$$

The formalism needs to be applied to all contributions of E [Sue99]. It results in defining of an effective magnetic field \mathbf{H}_{eff} by use of the energy density $\mathcal{E} = \frac{E}{V}$

$$\frac{1}{\mu_0 M_s} \frac{\delta \mathcal{E}}{\delta \mathbf{u}} = -\mathbf{H}_{eff} \quad (2.13)$$

with

$$\mathbf{H}_{eff} = \frac{2A}{\mu_0 M_s} \nabla^2 \mathbf{u} + \frac{2K_1}{\mu_0 M_s} (\mathbf{u} \cdot \mathbf{k}) \mathbf{k} + \mathbf{H}_{ext} \quad (2.14)$$

The minimum condition that needs to be fulfilled is

$$\mu_0 \mathbf{H}_{eff} \times \mathbf{M} = 0 \quad (2.15)$$

2.4 Finite Difference Method

The Gibb's Free Energy is a functional of the continuous magnetization distribution $\mathbf{M}(\mathbf{r})$. In the following chapters we will introduce a transition from the continuous magnetization to a system of discrete spin vectors, located on nodes of a grid. This semi-classical approach allows us to reduce the degrees of freedom of our system. Another feature that comes with the discretion of space is that differentials and gradients can be approximated by difference quotients. This approximation - in general - is only valid for small arguments. Many other and different procedures have been examined. The method of choice depends on a variety of properties such as, complexity of the geometry, the type of differential equation which is aimed to be solved, the accuracy ...

We will apply the procedure to the exchange energy [Sch06]. We start at 2.10 and replace the differential

2 Basics of Micromagnetism

$$\begin{aligned}
 (\nabla u_x)^2 &= \left(\frac{\partial u_x}{\partial x} \right)^2 + \left(\frac{\partial u_x}{\partial y} \right)^2 + \left(\frac{\partial u_x}{\partial z} \right)^2 \\
 &\rightarrow \left(\frac{\Delta_x u_x}{\Delta x} \right)^2 + \left(\frac{\Delta_y u_x}{\Delta y} \right)^2 + \left(\frac{\Delta_z u_x}{\Delta z} \right)^2
 \end{aligned} \tag{2.16}$$

with Δx being the distance between two lattice sites in x direction. For a regular cubic lattice it holds true that

$$\Delta x = \Delta y = \Delta z = a$$

Calculating the exchange of i -th and $i + 1$ -th spin explicitly, we write for the first term in 2.16

$$\begin{aligned}
 \left(\frac{\Delta u_x}{\Delta x} \right)^2 &= \frac{(u_{i+1,x} - u_{i,x})^2}{a^2} \\
 &= \frac{(u_{i+1,x}^2 - 2u_{i+1,x}u_{i,x} + u_{i,x}^2)}{a^2}
 \end{aligned} \tag{2.17}$$

Performing this on the other components and inserting the boundary condition $|\mathbf{u}| = 1$, while summing over the components, yields

$$\left(\frac{\Delta u_x}{\Delta x} \right)^2 = \frac{1}{a^2} (2 - 2\mathbf{u}_i \cdot \mathbf{u}_j) \tag{2.18}$$

Same procedure may be applied for the neighbor at site $i - 1$. Accounting for the double counting in the sum by dividing by 2, we obtain the discretized exchange energy.

$$\mathcal{E}_{sch} = \frac{A}{a^2} \sum_i [1 - (\mathbf{u}_i \cdot \mathbf{u}_{i+1} + \mathbf{u}_i \cdot \mathbf{u}_{i-1})] \tag{2.19}$$

We have set $A_{i,i-1} = A_{i,i+1} = A$

The anisotropy energy is

$$\mathcal{E}_{ani} = K_1 \sum_i (1 - (\mathbf{u}_i \cdot \mathbf{k}_i)^2) \tag{2.20}$$

3 Dynamical Analysis of Micromagnetics

In this chapter we will discuss the time evolution of a system consisting of a variable number of micromagnetic spin vectors. Each vector will be considered to have only two neighboring spins as though we were looking at a chain of spins. This will be of significance, especially when we motivate the exchange interaction between adjacent vectors. Different scenarios are simulated:

At first analytical formula for calculation of micromagnetic dynamics is discussed and simple examples of a 1-spin- and 3-spin-systems are given. Furthermore we investigate the absolute magnetization of 20 spins - which have identical anisotropy constants - that are exposed to a time dependent external magnetic field, which is inclined to the easy direction by 45° . We compare these results to a 80-spin-system where the first 40 spins have no anisotropy at all but the latter do, while the external field will be applied 1° off the easy axis.

3.1 Landau Lifschitz Gilbert Equation

The Landau Lifschitz Gilbert Equation (hereafter referred to as LLG) is a differential equation that describes dynamics of a magnetic system on a micromagnetic scale [Bro63b]. In the following we will briefly derive the LLG.

To start, we note that an external field \mathbf{H} applied to a magnetic moment μ results in a torque $\mu \times \mathbf{H}$. The torque is the derivative of the angular momentum \mathbf{L} with respect to time, hence

$$\frac{d}{dt}\mathbf{L} = \mu \times \mathbf{H} \quad (3.1)$$

Since we know that the magnetic moment μ and the angular momentum \mathbf{L} are connected to each other by the gyromagnetic ratio $\gamma = \frac{ge}{2m_e c}$, where g is the Landé factor, e is the elementary

3 Dynamical Analysis of Micromagnetics

charge, m_e is the electron mass, and c is the speed of light, we denote

$$\boldsymbol{\mu} = -\gamma \mathbf{L} \quad (3.2)$$

Taking both these identities into account we arrive at an expression that describes the time development of the magnetic moment $\boldsymbol{\mu}$

$$\frac{d}{dt}\boldsymbol{\mu} = -\gamma \boldsymbol{\mu} \times \mathbf{H} \quad (3.3)$$

In micromagnetics we replace the magnetic moment $\boldsymbol{\mu}$ by a continuous magnetization vector \mathbf{M} .

$$\frac{d}{dt}\mathbf{M} = -\gamma \mathbf{M} \times \mathbf{H} \quad (3.4)$$

This equation describes a precession - the so-called Larmor precession - of the magnetization vector \mathbf{M} around the field \mathbf{H} . If we look closely we realize that this equation may not lead to saturation of magnetization with increasing magnetic field, which would pose a radical inconsistency with experimental results like hysteresis curves. For this reason Gilbert proposed to alter it in 1955 by adding a phenomenological damping term, which could not be explained fundamentally but succeeded in conquering the inaccuracies the previous equation 3.4 offered. Inserting $\mathbf{J} = \mu_0 \mathbf{M}$ the Gilbert equation is

$$\frac{d}{dt}\mathbf{J} = -\gamma \mathbf{J} \times \mathbf{H} + \alpha \frac{\mathbf{J}}{J_s} \times \frac{d\mathbf{J}}{dt} \quad (3.5)$$

where J_s is the saturation polarization of the magnetic polarization vector \mathbf{J} and α is a dimensionless constant scaling the damping factor.

The damping term yields a vector that is perpendicular to the magnetic polarization \mathbf{J} and slowly pulls it towards the direction of the magnetic field vector \mathbf{H} until saturation is reached, hence polarization and field are parallel.

It is worth noting, that by expanding 3.5 by means of the scalar product with \mathbf{J} , we deduce that the saturation polarization J_s - and therefore also the saturation magnetization M_s - remains constant for all times.

$$\frac{d}{dt}J_s = 0 \quad (3.6)$$

The only step left is to isolate the differential operators from the other terms. In order to accomplish this we expand 3.5 by means of the vector product with \mathbf{J} . This leads to

$$\mathbf{J} \times \frac{d}{dt}\mathbf{J} = -\gamma\mathbf{J} \times (\mathbf{J} \times \mathbf{H}) + \alpha\mathbf{J} \times \left(\frac{\mathbf{J}}{J_s} \times \frac{d\mathbf{J}}{dt}\right) \quad (3.7)$$

$$\mathbf{J} \times \frac{d}{dt}\mathbf{J} = -\gamma\mathbf{J} \times (\mathbf{J} \times \mathbf{H}) - \alpha J_s \frac{d\mathbf{J}}{dt} \quad (3.8)$$

Inserting this result into 3.5 yields the Landau-Lifschitz-Gilbert Equation

$$\frac{d}{dt}\mathbf{J} = -\gamma'\mathbf{J} \times (\mathbf{J} \times \mathbf{H}) - \alpha\gamma'\frac{\mathbf{J}}{J_s} \times (\mathbf{J} \times \mathbf{H}) \quad (3.9)$$

where $\gamma' = \frac{\gamma}{1+\alpha^2}$.

The LLG is a differential equation of first order. Its first part describes a precession of the magnetic polarization vector \mathbf{J} around the magnetic field vector \mathbf{H} , the second part is the damping term, which can be interpreted as energy dissipation that ultimately leads to a parallel alignment of polarization and field vectors.

3.2 Solid Body Systems

3.2.1 Single Spin System

We consider a special case scenario where only one vector of magnetic polarization \mathbf{J} is present. We apply a magnetic field \mathbf{H}_{ext} along the cartesian z-axis.

In case of a real solid state body environment we have to take magnetocrystalline anisotropy into account. The anisotropy - as pointed out in the previous chapter - describes the fact that there are so-called 'easy'-directions which are energetically preferable for the polarization vector to point into, thus it makes it easier to magnetize the material along those directions. All simulations in this diploma thesis were done assuming that there is only one 'easy'-axis. In this example - for simplicity - we let the 'easy'-axis unit vector \mathbf{k} be parallel to the magnetic field \mathbf{H}_{ext} .

If we remind ourselves of the structure of the LLG 3.9, we notice that it is no longer sufficient to consider \mathbf{H}_{ext} . To describe the physics of this system correctly, we have to substitute the magnetic field \mathbf{H} by an effective field \mathbf{H}_{eff} that takes anisotropy into account as well as the

3 Dynamical Analysis of Micromagnetics

external field \mathbf{H}_{ext} . We therefore write 3.9 in the form

$$\frac{d}{dt}\mathbf{J} = -\gamma'\mathbf{J} \times (\mathbf{J} \times \mathbf{H}_{eff}) - \alpha\gamma'\frac{\mathbf{J}}{J_s} \times (\mathbf{J} \times \mathbf{H}_{eff}) \quad (3.10)$$

with

$$\mathbf{H}_{eff} = \mathbf{H}_{ext} + \mathbf{H}_{ani} \quad (3.11)$$

and using $\mathbf{u} = \frac{1}{J_s}\mathbf{J}$

$$\mathbf{H}_{ani} = \frac{2K_1}{J_s}(\mathbf{u} \cdot \mathbf{k})\mathbf{k} \quad (3.12)$$

where K_1 is the anisotropy constant [Sue99].

In order to start our simulation we need to provide a starting position of our polarization vector \mathbf{J} . In this case we set the initial coordinates to $\mathbf{J} = (0, 1, 0)$, so the polarization \mathbf{J} points into positive y-direction within three-dimensional cartesian space and the saturation polarization is $J_s = 1T$. The damping constant is $\alpha = 0.1$, the anisotropy constant is $K_1 = 10^6 Jm^{-3}$, and $\mathbf{H}_{ext} = \mathbf{k} = (0, 0, 1)$.

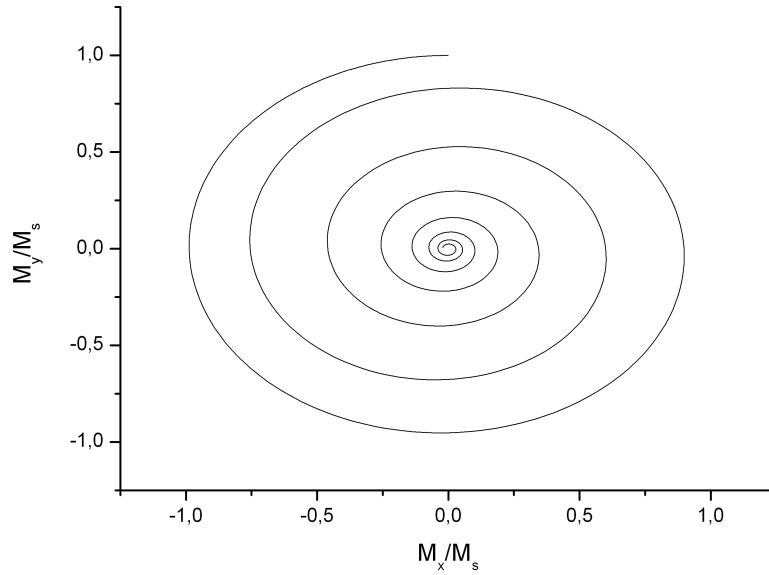


Figure 3.1: trajectory of single spin in m_x, m_y -plane with $\mathbf{k} \parallel \mathbf{H}_{ext}$

3.1 shows the trajectory of a single polarization vector in the cartesian x,y-plane. Since the applied magnetic field \mathbf{H} is parallel to the 'easy'-axis unit vector \mathbf{k} , \mathbf{H}_{eff} is parallel as well, and we observe the predicted behavior of the polarization precessing about the effective field, but also being pulled towards it by the damping term in 3.10.

If we change the 'easy'-direction to something different, e.g. $\mathbf{k} = (\vartheta_k, \varphi_k) = \frac{1}{7}(\pi, \pi)$ we find an analogous solution 3.2.

We note that by changing the 'easy'-direction \mathbf{k} , we ultimately change the minimum direction,

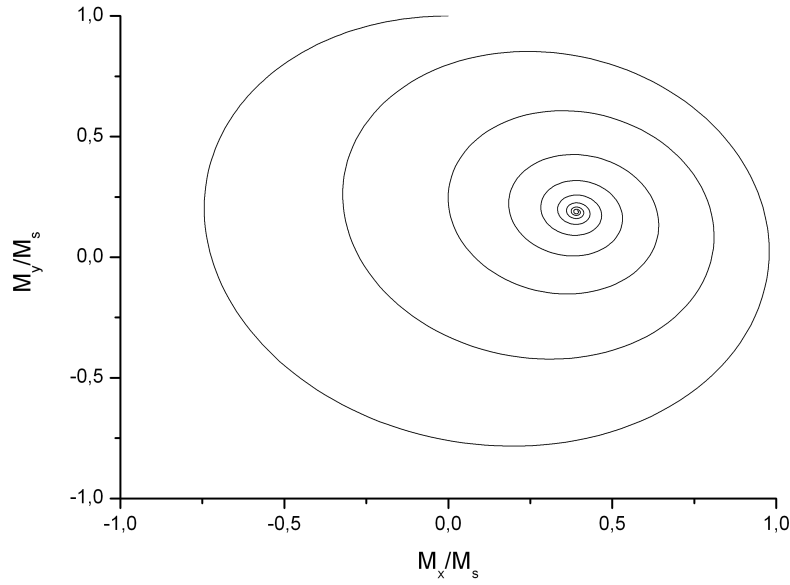


Figure 3.2: single spin trajectory with \mathbf{k} and \mathbf{H}_{ext} not parallel

into which the system converges. The same would hold true, of course, if we were to change the direction of the external magnetic field \mathbf{H}_{ext} .

3.2.2 3 Spin System

In this section we will add two more spins to our system, creating a 3-spin-chain. Again we apply an external magnetic field parallel to the z-axis, which we also choose to be the 'easy'-direction. Since we are now looking at a multi-spin-system we have to respect the exchange interaction between the spins. Once again we alter the effective field \mathbf{H}_{eff} by adding another

3 Dynamical Analysis of Micromagnetics

term \mathbf{H}_{xch} such that

$$\mathbf{H}_{eff,i} = \mathbf{H}_{ext,i} + \mathbf{H}_{ani,i} + \mathbf{H}_{xch,i} \quad (3.13)$$

where $\mathbf{H}_{eff,i}$ is the effective magnetic field acting on the i -th polarization vector, with

$$\mathbf{H}_{xch,i} = \frac{2A}{J_s a^2} \sum_{NN} \mathbf{u}_j \quad (3.14)$$

where A is the exchange constant and a is the distance between two neighboring spins. The sum is to be taken over nearest neighbors only.

For $A = 10^{-11} \frac{J}{m}$ and $a = 1nm$ we find 3.3

Clearly, the three spins act as though they were strongly connected to each other, moving in

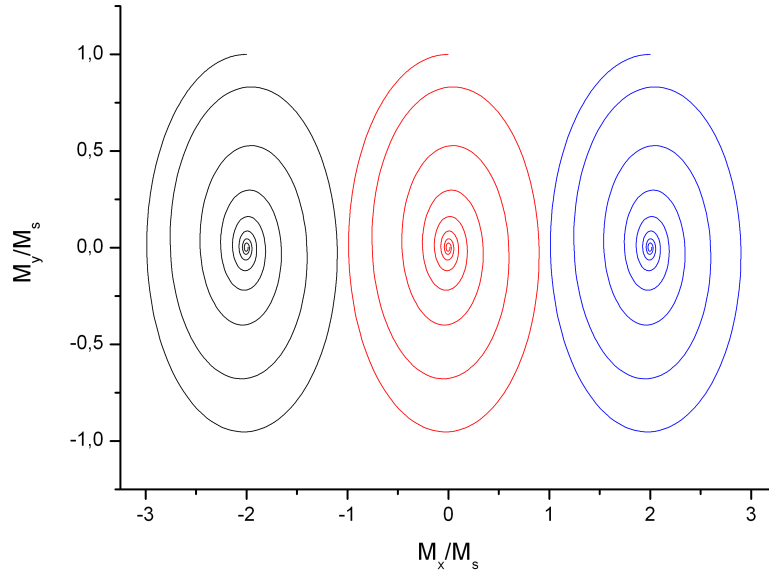


Figure 3.3: trajectories of three interacting spins with $\mathbf{k} \parallel \mathbf{H}_{ext}$

unimotion. This result is not surprising, due to the structure of the LLG and \mathbf{H}_{eff} . It is also noteworthy that the exchange interaction does not change the direction, which the spins are pointing into, for the minimum configuration. It is merely a scaling factor of how strongly they are correlated. This means that in a solid state body the exchange interaction between electrons does not prefer one specific polarization direction over the other, it leaves the magnetic order isotropic. Comparing 3.3 to 3.2 we deduce that, in absence of an external magnetic field

\mathbf{H}_{ext} , the only contribution to the effective field \mathbf{H}_{eff} , that makes one polarization direction preferable to the other - and therefore destroys isotropy - , is the magnetocrystalline anisotropy (hence the name).

3.3 Magnetization Alteration Analysis

The recording process of data - and therefore data storage as a whole - can only be provided if the magnetization in regions, where the information is intended to be written, can be switched reproducibly. In the previous sections we have discussed how magnetic fields influence the dynamics of magnetic spins and how different contributions add to the LLG through the effective magnetic field \mathbf{H}_{eff} in 3.10. We have observed that eventually the magnetization converges into a stable state, a local minimum of the system's Gibb's Free Energy E .

However, there is no immediate indication that this needs to be the only local minimum state available and there might be other (meta)stable states possible to reach. Such states can be obtained, for example, by applying very strong external fields in order to force the system into another local minimum state, where it may prevail for some time. It needs to be pointed out that such a transition may happen on its own due to thermal activity. In this section we will omit such transitions and idealize the model by defining $T = 0$. The influence of temperature on the stability of a magnetization state will be tackled later.

Recording media are made up out of much larger clusters of spins, but can qualitatively be described by long spin chains. 3.3 has shown that a local set of spins will act in unimotion, because of the strong exchange interaction between them. Hence, - neglecting boundary problems - we expect spins in a whole cluster to act in unimotion as well and by summing over all polarization vectors within the cluster, we obtain a vector, that represents the whole cluster. Such a cluster with two potential minimum configurations (e.g. *spin – up* and *spin – down*) can be interpreted as an entity of information; a bit.

In recent years questions have arisen how large this clusters have to be in order to be able to neglect surface problems but maintain product quality. Obviously surface contributions increase with decreasing cluster size, which affect stability [Sch09].

3.3.1 40 Spin System

We will start with a chain of 40 spins. The 'easy'-direction is once again $\mathbf{k} = (0, 0, 1)$, and the initial configuration sees all spins pointing into the 'easy'-direction. The system is already in an energetic minimum.

We will now switch on an external magnetic field that is inclined by $\xi = 45^\circ$ against the easy axis. We vary the magnitude of the external field H_{ext} over a range of $[-4, 4] \frac{K_1}{J_s}$ and measure the magnetization along the z-axis. For $A = 10^{-11} \frac{A}{m}$, $a = 1nm$, $K_1 = 10^6 Jm^{-3}$, $J_s = \frac{1}{2}T$, and $\alpha = 1$ we find 3.4

Initially the magnetization is in saturation $M_z = M_s$, since all polarization vectors point into

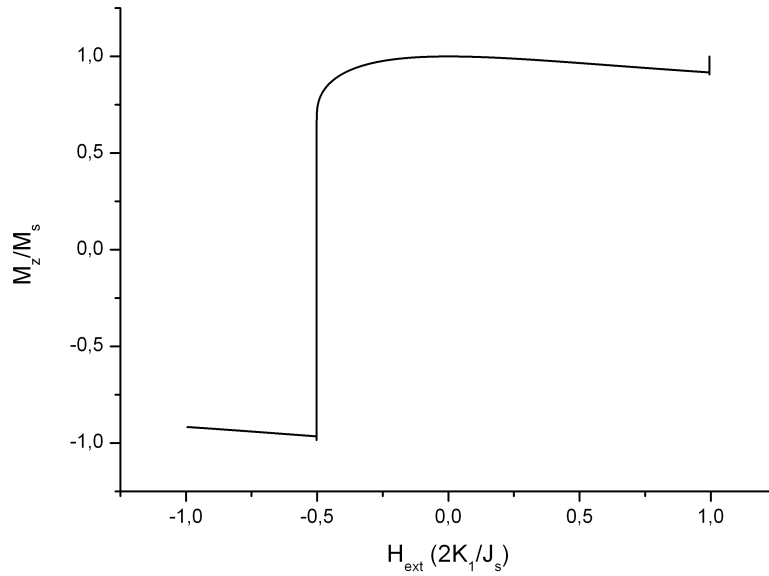


Figure 3.4: magnetization over external field

the same direction. Once the external field is turned on, the minimum configuration changes and M_z decreases, because the other magnetization components change to $M_x \neq 0$ and $M_y \neq 0$. At a critical magnitude of $H_{ext} = H_c = -\frac{K_1}{J_s}$ there is a sudden reversal of magnetization, where spins flip over and $M_z = -M_s$. This flip over could be interpreted as a writing process on a hard disc, turning a bit from 0 to 1. As we can see the critical (=coercivity) field H_c , that needs to be provided in order to change the polarization configuration, is proportional to the anisotropy constant K_1 .

3.3.2 2×40 Spin System

We go on to another chain of spins. This time we look at a chain of 80 polarization vectors, the first 40 of which shall have no anisotropy, the latter are equal to the ones described in the previous section. The external field will be varied as in the previous section, but with an inclination of $\xi = 1^\circ$ against the 'easy'-direction. For the usual set of constants we find 3.5.

At first glance we see a strong resemblance to 3.4, but the spin flip has a somewhat inhar-

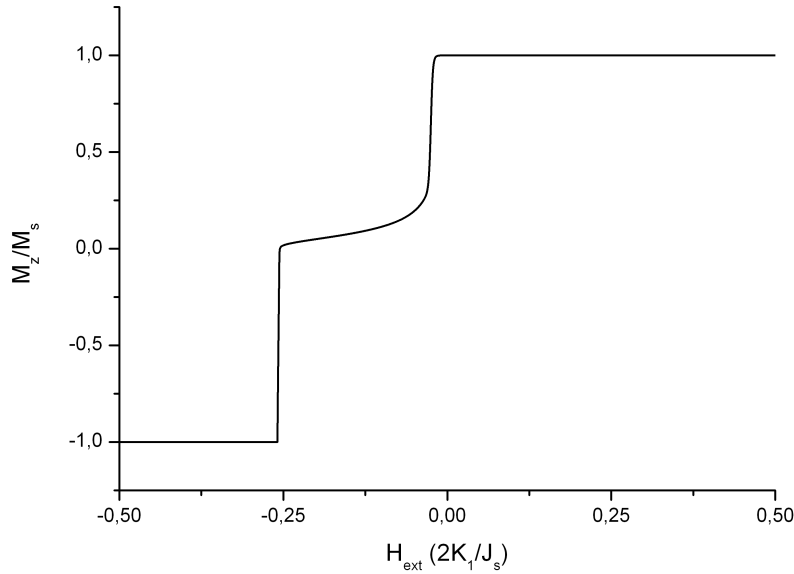


Figure 3.5: magnetization over external field

monious feature to it. Once more we measure saturation for no externally applied field, and due to the fact that this time the inclination between applied field and 'easy'-axis is very little, this saturation upholds even for higher magnitudes of \mathbf{H}_{ext} . Once we turn the magnetic field against the 'easy'-direction, we see an immediate response in the magnetization. It originates from the first 40 spins which are not affected by anisotropy. The only contributions to \mathbf{H}_{eff} for those spins are \mathbf{H}_{xch} and \mathbf{H}_{ext} . Since \mathbf{H}_{ext} changes sign, they attempt immediate spin flips, but \mathbf{H}_{xch} conquers the flipping for the ones nearest to the set of anisotropically interacting spins, because - in our simulation - the exchange interaction favors ferromagnetic (parallel) alignment of spins. Nevertheless, for a critical field $H_c = -\frac{K_1}{2J_s}$ the anisotropic contribution to \mathbf{H}_{eff} for the latter spins is overpowered and they perform the flip as well.

We will take a look at the flipping motion in a little more detail. 3.6 to 3.9 qualitatively show

the development of a Bloch wall for $H_c < H_{ext} < 0$ as a result of the competition between exchange interaction and anisotropy energy. Colors represent values of M_z .

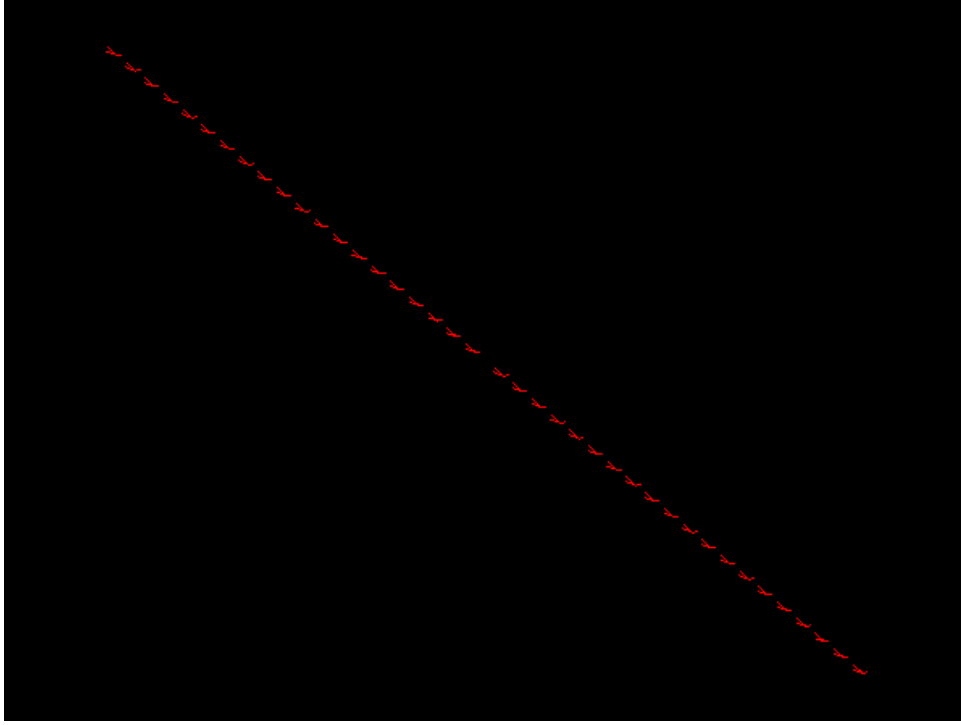


Figure 3.6: spin chain for $H_{ext} = 0$

3.3.3 Conclusion

Clearly the stability of a magnetization state is closely related to the magnitude of the anisotropy constant K_1 . Simply put, if one magnetization direction is much more preferable to all others in its vicinity, it is even harder to change the particle's spin orientation. This should mean that for recording media, it is on the one hand a great feat to use materials that provide a high K_1 -value, because it adds to the stability of the system, but on the other hand it makes writing processes very energy consuming, since along with increasing stability there comes an increasing coercivity field H_c . Along with the urge of developing ever smaller entities of information to get a good signal-to-noise ratio and the henceforth arising vulnerability of a magnetization state to temperature, we name the trilemma of magnetic recording [Sch09].

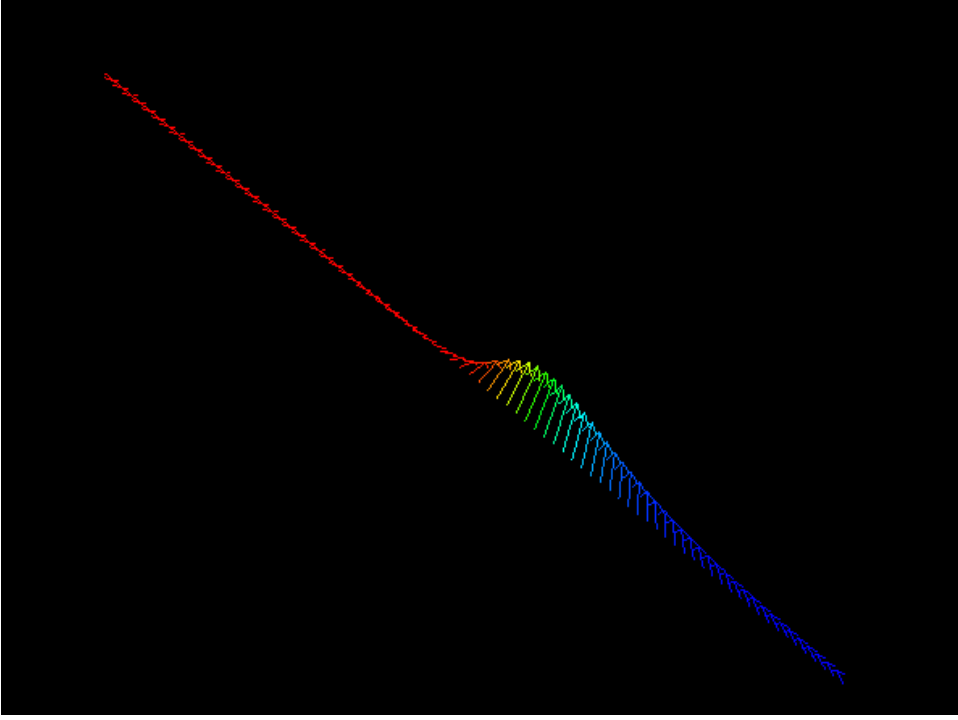


Figure 3.7: $H_{ext} = -0.1 \frac{2K_1}{J_s}$

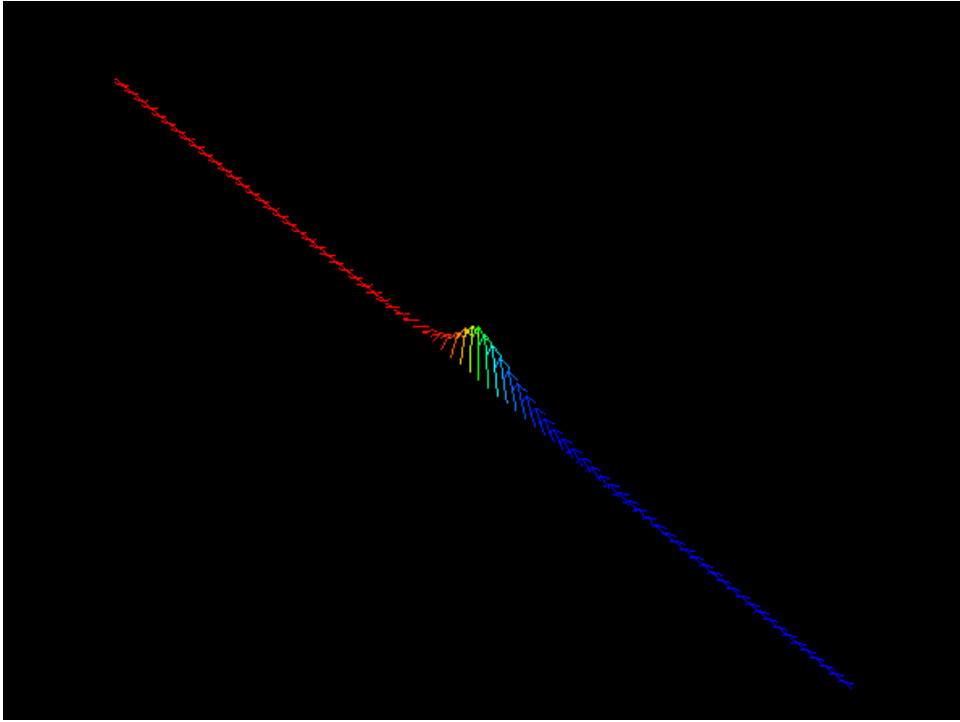


Figure 3.8: $H_{ext} = -0.22 \frac{2K_1}{J_s}$

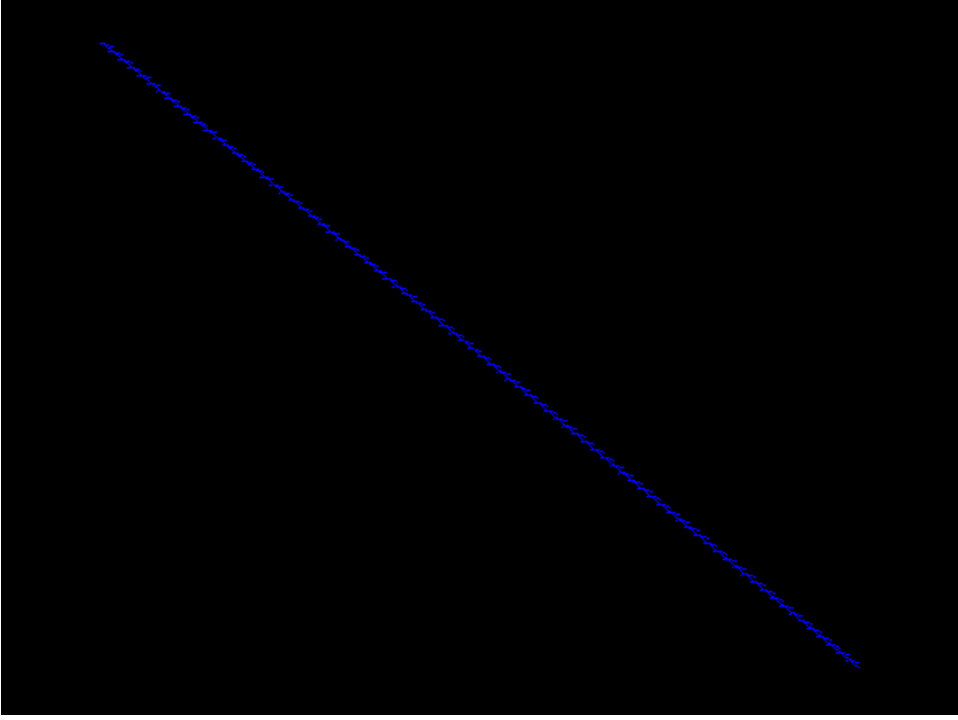


Figure 3.9: $H_{ext} = -0.3 \frac{2K_1}{J_s}$

4 Analytical Calculation of the Attempt Frequency

4.1 Thoughts on Stability

It was already discussed, that minimization of the Gibb's Free Energy leads to a magnetization distribution of equilibrium. However, there might be multiple possible configurations that would minimize E at least locally. This means that in principle there are many (meta)stable states that can be occupied, which are parted by maxima or saddle-points of the Gibb's Free Energy. The analysis of stability of a system is analogous to answering the question of how likely the system is to make a transition from one local minimum to the other.

In the previous chapter we have seen that a system always converges into equilibrium, and implicitly we expected it to stay there, once it has reached it. So the question arises why it even should suddenly change from one minimum configuration to the other. The answer is thermal activity.

In the previous chapter we restricted our system to $T = 0$ and therefore had a completely deterministic model to work with. To introduce thermal activity ($T > 0$) to our system we would have to add a stochastic variable (a stochastic field \mathbf{H}_{th}) to the LLG 3.10 as was done in [Sch09].

W.F. Brown [Bro63a] and L. Néel [Né49] are accountable for the predominantly used theory on this field. Brown found a Fokker-Plank-Equation to describe a distribution function to tackle this problem and by applying it to an idea by Kramers [Kra40]. Kramers developed the transition state theory in order to estimate the rate constant between stable states.

4.2 Attempt Frequency

The attempt frequency is a measure of how stable a magnetic state is. It describes how likely a system performs a sudden transition into another state of local energetic minimum. Braun [Bra94] and Langer [Lan67] explained the attempt frequency as a measure of the total probability current of a stationary non-equilibrium magnetization state through a surface near the saddle-point. An empirical equation to describe a transition like this, was proposed by the chemist Arrhenius.

$$f = f_0 e^{-\frac{\Delta E}{k_B T}} \quad (4.1)$$

where f is the rate of magnetization reversal, f_0 is the attempt frequency, T the absolute temperature, k_B is the Boltzmann constant, and ΔE is the energy barrier that needs to be overcome to switch from the initial state to the final state. Initially, 4.1 was designed to explain the temperature dependency of chemical reactions frequencies, but Néel applied it to the problems of micromagnetism. We can see that f increases with increasing T , while a higher energy barrier ΔE results in a lesser rate. Intuitively this is plausible, because a higher energy barrier should make a rather more stable state. Methods of calculating the energy barrier are given in [EPCF08] [RDF02]. The temperature dependence of f is isolated within the exponential function, leaving the attempt frequency temperature independent. In general, this need not hold true. Braun proposed a way to derive the attempt frequency [Bra94]. He arrived at

$$f_0 = \frac{\lambda_+ \Omega_0}{2\pi} \quad (4.2)$$

so f_0 is composed of a product of two factors Ω_0 and λ_+ . The statistical prefactor Ω_0 is proportional to the configuration's volume in phase space, whereas λ_+ is the dynamical factor and results from the LLG [Bra94].

4.3 The Statistical Prefactor Ω_0

In order to be able to calculate Ω_0 , we need to derive the second derivative of the Gibb's Free Energy at each spin with respect to the set of spherical coordinates (ϑ, φ) , and evaluate the

resulting Hessian at the minimum configuration and at the saddle-point [Bra94].

$$\Omega_0 = \sqrt{\frac{\det H_{min}}{|\det H_{sad}|}} \quad (4.3)$$

with

$$H_{min} = \begin{pmatrix} \frac{\partial^2 E}{\partial \vartheta^2} & \frac{\partial^2 E}{\partial \vartheta \partial \varphi} \\ \frac{\partial^2 E}{\partial \vartheta \partial \varphi} & \frac{\partial^2 E}{\partial \varphi^2} \end{pmatrix}_{min} \quad (4.4)$$

4.4 Spherical Hessian

Our objective is to derive the second spherical derivative of the Gibb's Free Energy, without transforming the expression for E itself into spherical coordinates. In this section we will derive an analytical formalism to transform the Hessian Matrix $\hat{H}_{x,y,z}$

$$\hat{H}_{x,y,z} = \begin{pmatrix} \frac{\partial^2 E}{\partial u_x^2} & \frac{\partial^2 E}{\partial u_x \partial u_y} & \frac{\partial^2 E}{\partial u_x \partial u_z} \\ \frac{\partial^2 E}{\partial u_y \partial u_x} & \frac{\partial^2 E}{\partial u_y^2} & \frac{\partial^2 E}{\partial u_y \partial u_z} \\ \frac{\partial^2 E}{\partial u_z \partial u_x} & \frac{\partial^2 E}{\partial u_z \partial u_y} & \frac{\partial^2 E}{\partial u_z^2} \end{pmatrix} \quad (4.5)$$

which contains derivatives with respect to the cartesian components of the polarization vectors \mathbf{J}_i , into a spherical Hessian $\hat{H}_{\vartheta,\varphi}$, that contains derivatives with respect to the spherical coordinates ϑ_i , φ_i . Although we do not account for the radial derivative $\frac{\partial}{\partial r}$ we do not lose any information, owing to the fact that for all polarization vectors it holds true that $|\mathbf{J}| = J_s$ and therefore $r = J_s = \text{const}$. By deriving the transforming algorithm of the cartesian 3×3 -Hessian $\hat{H}_{x,y,z}$ into a spherical 2×2 -Hessian $\hat{H}_{\vartheta,\varphi}$ for each lattice site (i.e. spin), we will obtain a formalism that allows us to keep the cartesian expression for the Gibb's Free Energy, and still use the spherical derivative to calculate Ω_0 .

For any coordinate transformation differential operators are connected such that

4 Analytical Calculation of the Attempt Frequency

$$\begin{aligned}
\frac{\partial}{\partial a_{i,\alpha}} &= \frac{\partial b_{n,\alpha}}{\partial a_{i,\alpha}} \frac{\partial}{\partial b_{n,\alpha}} \\
\frac{\partial}{\partial a_{i,\alpha}} \frac{\partial}{\partial a_{j,\beta}} &= \frac{\partial b_{n,\alpha}}{\partial a_{i,\alpha}} \frac{\partial}{\partial b_{n,\alpha}} \frac{\partial b_{m,\beta}}{\partial a_{j,\beta}} \frac{\partial}{\partial b_{m,\beta}} \\
&= \frac{\partial b_{n,\alpha}}{\partial a_{i,\alpha}} \left[\left(\frac{\partial}{\partial b_{n,\alpha}} \frac{\partial b_{m,\beta}}{\partial a_{j,\beta}} \right) \frac{\partial}{\partial b_{m,\beta}} + \frac{\partial b_{m,\beta}}{\partial a_{j,\beta}} \frac{\partial^2}{\partial b_{n,\alpha} \partial b_{m,\beta}} \right]
\end{aligned} \tag{4.6}$$

where - for our purposes - letters a, b represent a set of coordinates, Latin indices sum over coordinates (e.g. $a_i = \vartheta, \varphi$ and $b_m = x, y, z$), and Greek indices label different spins ($\alpha, \beta = 1, 2, 3, \dots$). Note that Einstein's sum convention does only apply to Latin indices i, j and not to Greek ones. For now we let α, β be free indices, which may not be subject to summation. We try to indicate discrepancies in meaning and handling, in relation to i, j by putting a comma in between them, like in 4.6.

We expand the term in the round brackets

$$\begin{aligned}
\frac{\partial}{\partial b_{n,\alpha}} \frac{\partial b_{m,\beta}}{\partial a_{j,\beta}} &= \frac{\partial a_{i,\alpha}}{\partial b_{n,\alpha}} \frac{\partial}{\partial a_{i,\alpha}} \frac{\partial b_{m,\beta}}{\partial a_{j,\beta}} \\
&= \frac{\partial a_{i,\alpha}}{\partial b_{n,\alpha}} \frac{\partial^2 b_{m,\beta}}{\partial a_{i,\alpha} \partial a_{j,\beta}}
\end{aligned} \tag{4.7}$$

Since the partial derivatives with respect to coordinates on two different sites are not connected, the last term in 4.7 is only nonzero, if $\alpha = \beta$. This simplifies explicit calculation immensely, because the following tensor product with $\frac{\partial}{\partial b_{m,\beta}}$ is reduced to a scalar product of two vectors, and our notation convention concerning indices is not threatened. We therefore add a Kronecker symbol $\delta_{\alpha\beta}$, which for $\alpha = \beta$ is 1 and else 0, to 4.7, and insert the result into 4.6. This yields

$$\frac{\partial}{\partial a_{i,\alpha}} \frac{\partial}{\partial a_{j,\beta}} = \delta_{\alpha\beta} \frac{\partial^2 b_{m,\beta}}{\partial a_{i,\alpha} \partial a_{j,\beta}} \frac{\partial}{\partial b_{m,\beta}} + \frac{\partial b_{n,\alpha}}{\partial a_{i,\alpha}} \frac{\partial b_{m,\beta}}{\partial a_{j,\beta}} \frac{\partial^2}{\partial b_{n,\alpha} \partial b_{m,\beta}} \tag{4.8}$$

On the left hand side of 4.8 we count 4 free indices, that - if we were to apply Einstein's sum convention regularly - would define a 4th-grade tensor $\hat{t}_{i,j,\alpha,\beta}$. However in our notation, for arbitrary number of spins N and $i, j = 1, \dots, q$, let $\hat{T}_{\{a_i\}}^N$ be a $Nq \times Nq$ matrix, e.g. for $q = 2$ and $N = 1$

$$\hat{T}_{\{\vartheta, \varphi\}}^1 = \begin{pmatrix} \frac{\partial^2}{\partial \vartheta^2} & \frac{\partial^2}{\partial \vartheta \partial \varphi} \\ \frac{\partial^2}{\partial \vartheta \partial \varphi} & \frac{\partial^2}{\partial \varphi^2} \end{pmatrix} \quad (4.9)$$

and $N = q = 2$

$$\hat{T}_{\{\vartheta, \varphi\}}^2 = \begin{pmatrix} \frac{\partial^2}{\partial \vartheta_1^2} & \frac{\partial^2}{\partial \vartheta_1 \partial \varphi_1} & \frac{\partial^2}{\partial \vartheta_1 \partial \vartheta_2} & \frac{\partial^2}{\partial \vartheta_1 \partial \varphi_2} \\ \frac{\partial^2}{\partial \vartheta_1 \partial \varphi_1} & \frac{\partial^2}{\partial \varphi_1^2} & \frac{\partial^2}{\partial \vartheta_2 \partial \varphi_1} & \frac{\partial^2}{\partial \varphi_1 \partial \varphi_2} \\ \frac{\partial^2}{\partial \vartheta_2 \partial \vartheta_1} & \frac{\partial^2}{\partial \vartheta_2 \partial \varphi_1} & \frac{\partial^2}{\partial \vartheta_2^2} & \frac{\partial^2}{\partial \vartheta_2 \partial \varphi_2} \\ \frac{\partial^2}{\partial \vartheta_1 \partial \varphi_2} & \frac{\partial^2}{\partial \varphi_2 \partial \varphi_1} & \frac{\partial^2}{\partial \vartheta_2 \partial \varphi_2} & \frac{\partial^2}{\partial \varphi_2^2} \end{pmatrix} \quad (4.10)$$

4.5 Single Spin System

4.5.1 Single Spin Spherical Hessian

We apply the $\hat{T}_{\{a_i\}}^N$ -operator onto Gibb's Free Energy E of a single magnetic body ($q = 1$) and find

$$\hat{T}_{\{\vartheta, \varphi\}}^1 E = \hat{H}_{\vartheta, \varphi} = \begin{pmatrix} \frac{\partial^2 E}{\partial \vartheta^2} & \frac{\partial^2 E}{\partial \vartheta \partial \varphi} \\ \frac{\partial^2 E}{\partial \vartheta \partial \varphi} & \frac{\partial^2 E}{\partial \varphi^2} \end{pmatrix} \quad (4.11)$$

Following the rule 4.8 we arrive at expressions for the components of the matrix $\hat{H}_{\vartheta, \varphi}$. Shuffling terms around we finally arrive at

4 Analytical Calculation of the Attempt Frequency

$$\frac{\partial^2 E}{\partial \vartheta^2} = \left[\begin{pmatrix} \frac{\partial^2 E}{\partial u_x^2} & \frac{\partial^2 E}{\partial u_x \partial u_y} & \frac{\partial^2 E}{\partial u_x \partial u_z} \\ \frac{\partial^2 E}{\partial u_y \partial u_x} & \frac{\partial^2 E}{\partial u_y^2} & \frac{\partial^2 E}{\partial u_y \partial u_z} \\ \frac{\partial^2 E}{\partial u_z \partial u_x} & \frac{\partial^2 E}{\partial u_z \partial u_y} & \frac{\partial^2 E}{\partial u_z^2} \end{pmatrix} \begin{pmatrix} \frac{\partial u_x}{\partial \vartheta} \\ \frac{\partial u_y}{\partial \vartheta} \\ \frac{\partial u_z}{\partial \vartheta} \end{pmatrix} \right] \cdot \begin{pmatrix} \frac{\partial u_x}{\partial \vartheta} \\ \frac{\partial u_y}{\partial \vartheta} \\ \frac{\partial u_z}{\partial \vartheta} \end{pmatrix} + \begin{pmatrix} \frac{\partial^2 u_x}{\partial \vartheta^2} \\ \frac{\partial^2 u_y}{\partial \vartheta^2} \\ \frac{\partial^2 u_z}{\partial \vartheta^2} \end{pmatrix} \cdot \begin{pmatrix} \frac{\partial E}{\partial u_x} \\ \frac{\partial E}{\partial u_y} \\ \frac{\partial E}{\partial u_z} \end{pmatrix} \quad (4.12)$$

$$\frac{\partial^2 E}{\partial \varphi^2} = \left[\begin{pmatrix} \frac{\partial^2 E}{\partial u_x^2} & \frac{\partial^2 E}{\partial u_x \partial u_y} & \frac{\partial^2 E}{\partial u_x \partial u_z} \\ \frac{\partial^2 E}{\partial u_y \partial u_x} & \frac{\partial^2 E}{\partial u_y^2} & \frac{\partial^2 E}{\partial u_y \partial u_z} \\ \frac{\partial^2 E}{\partial u_z \partial u_x} & \frac{\partial^2 E}{\partial u_z \partial u_y} & \frac{\partial^2 E}{\partial u_z^2} \end{pmatrix} \begin{pmatrix} \frac{\partial u_x}{\partial \varphi} \\ \frac{\partial u_y}{\partial \varphi} \\ \frac{\partial u_z}{\partial \varphi} \end{pmatrix} \right] \cdot \begin{pmatrix} \frac{\partial u_x}{\partial \varphi} \\ \frac{\partial u_y}{\partial \varphi} \\ \frac{\partial u_z}{\partial \varphi} \end{pmatrix} + \begin{pmatrix} \frac{\partial^2 u_x}{\partial \varphi^2} \\ \frac{\partial^2 u_y}{\partial \varphi^2} \\ \frac{\partial^2 u_z}{\partial \varphi^2} \end{pmatrix} \cdot \begin{pmatrix} \frac{\partial E}{\partial u_x} \\ \frac{\partial E}{\partial u_y} \\ \frac{\partial E}{\partial u_z} \end{pmatrix} \quad (4.13)$$

$$\frac{\partial^2 E}{\partial \vartheta \partial \varphi} = \left[\begin{pmatrix} \frac{\partial^2 E}{\partial u_x^2} & \frac{\partial^2 E}{\partial u_x \partial u_y} & \frac{\partial^2 E}{\partial u_x \partial u_z} \\ \frac{\partial^2 E}{\partial u_y \partial u_x} & \frac{\partial^2 E}{\partial u_y^2} & \frac{\partial^2 E}{\partial u_y \partial u_z} \\ \frac{\partial^2 E}{\partial u_z \partial u_x} & \frac{\partial^2 E}{\partial u_z \partial u_y} & \frac{\partial^2 E}{\partial u_z^2} \end{pmatrix} \begin{pmatrix} \frac{\partial u_x}{\partial \vartheta} \\ \frac{\partial u_y}{\partial \vartheta} \\ \frac{\partial u_z}{\partial \vartheta} \end{pmatrix} \right] \cdot \begin{pmatrix} \frac{\partial u_x}{\partial \varphi} \\ \frac{\partial u_y}{\partial \varphi} \\ \frac{\partial u_z}{\partial \varphi} \end{pmatrix} + \begin{pmatrix} \frac{\partial^2 u_x}{\partial \vartheta \partial \varphi} \\ \frac{\partial^2 u_y}{\partial \vartheta \partial \varphi} \\ \frac{\partial^2 u_z}{\partial \vartheta \partial \varphi} \end{pmatrix} \cdot \begin{pmatrix} \frac{\partial E}{\partial u_x} \\ \frac{\partial E}{\partial u_y} \\ \frac{\partial E}{\partial u_z} \end{pmatrix} \quad (4.14)$$

Using the fact that the functional derivative of the Gibb's Free Energy E with respect to the magnetic polarization \mathbf{J} is the negative effective magnetic field \mathbf{H}_{eff}

$$\frac{\delta E}{\delta \mathbf{J}} = -\mathbf{H}_{eff} \quad (4.15)$$

and

$$-J_s \frac{\partial \mathbf{H}_{eff}}{\partial \mathbf{J}} = \begin{pmatrix} \frac{\partial^2 E}{\partial u_x^2} & \frac{\partial^2 E}{\partial u_x \partial u_y} & \frac{\partial^2 E}{\partial u_x \partial u_z} \\ \frac{\partial^2 E}{\partial u_y \partial u_x} & \frac{\partial^2 E}{\partial u_y^2} & \frac{\partial^2 E}{\partial u_y \partial u_z} \\ \frac{\partial^2 E}{\partial u_z \partial u_x} & \frac{\partial^2 E}{\partial u_z \partial u_y} & \frac{\partial^2 E}{\partial u_z^2} \end{pmatrix} \quad (4.16)$$

as well as

$$\begin{pmatrix} \frac{\partial u_x}{\partial \vartheta} \\ \frac{\partial u_y}{\partial \vartheta} \\ \frac{\partial u_z}{\partial \vartheta} \end{pmatrix} = \frac{1}{J_s} \frac{\partial \mathbf{J}}{\partial \vartheta} \quad (4.17)$$

we rewrite the first component of $\hat{H}_{\vartheta,\varphi}$

$$\frac{\partial^2 E}{\partial \vartheta^2} = \left[\left(-\frac{\partial \mathbf{H}_{eff}}{\partial \mathbf{J}} \right) \frac{\partial \mathbf{J}}{\partial \vartheta} \right] \cdot \frac{\partial \mathbf{J}}{\partial \vartheta} - \frac{\partial^2 \mathbf{J}}{\partial \vartheta^2} \cdot \mathbf{H}_{eff} \quad (4.18)$$

To calculate Ω_0 it is sufficient to have knowledge of \mathbf{H}_{eff} and its dependency on \mathbf{J} , as well as the magnetization itself. For the single spin system we have already shown, that there are only two contributions to \mathbf{H}_{eff} - the external field \mathbf{H}_{ext} and the crystalline anisotropy term \mathbf{H}_{ani} . Since \mathbf{H}_{ext} is not a function of \mathbf{J} , the first term in 4.18 features only contributions of the anisotropy field.

It is evident that $\hat{H}_{\vartheta,\varphi}$ is symmetric since

$$\frac{\partial^2 E}{\partial \vartheta \partial \varphi} = \frac{\partial^2 E}{\partial \varphi \partial \vartheta} \quad (4.19)$$

Hence all eigenvalues - and therefore determinants as well - of $\hat{H}_{\vartheta,\varphi}$ for both minimum and saddlepoint configurations are real.

4.5.2 Minimum and Saddle-Point Configurations

In the previous chapter we have seen, that for ferromagnetic coupling of the exchange interaction makes spins align parallel to each other. We can therefore assume that for minimum and saddle-point configurations, the lateral dimension of the spin chain is sufficient small, so that the particle can be regarded as single domain.

However, the information gained from spherical derivatives of vectors depends strongly on where on the surface of the sphere the derivation was carried out. Consider a derivation on one of the poles; e.g. $\vartheta = 0$. Since a change of the azimuth angle φ would result in no change of orientation, every derivative with respect to φ would equal zero.

To guarantee comparable results, we have to make sure that we carry out the derivations at sites that are in the vicinity of the x,y -plane. This restriction demands $\vartheta = \frac{\pi}{2}$. Effectively this means, that any minimum and saddle-point configurations must be transposed to fit on this plane. Such a transformation is well defined. Consider a sphere of radius $r = J_s$ and centered at $M = (0,0,0)$. The polarization vector \mathbf{J} may point from the center of the sphere onto the surface. Polarization vectors for minimum and saddle-point configurations define two points

P, Q on the surface. It is always possible to find a plane A through M , such that P, Q are elements of that plane. Following this definition [DB99] the crossing of such a plane with the corresponding sphere results in a great circle, that must feature P, Q . The transformation may now turn coordinate axis, such that the plane A becomes the x, y -plane and the great circle becomes the equator.

Such a transformation results in $\vartheta_{min} = \vartheta_{sad} = \frac{\pi}{2}$. The two configurations differ in their setting of the azimuth angle $\varphi_{min} \neq \varphi_{sad}$.

4.5.3 Explicit Calculation

We realize the right configurations for minimum and saddle-point by choosing the x -axis as 'easy'-direction and applying an external field parallel to the y -axis. The magnitude of \mathbf{H}_{ext} is measured by means of $h = \frac{H_{ext} J_s}{2K_1}$, making h a dimensionless parameter [Sch09]. This leads to a simple expression for Gibb's Free Energy

$$E = -VK_1 (\sin^2 \vartheta \cos^2 \varphi + 2h \sin \vartheta \sin \varphi) \quad (4.20)$$

and

$$\begin{aligned} \vartheta_{min} &= \frac{\pi}{2} & \varphi_{min} &= \pm \arcsin h \\ \vartheta_{sad} &= \frac{\pi}{2} & \varphi_{sad} &= \frac{\pi}{2} \end{aligned} \quad (4.21)$$

For the spherical Hessians we find

$$\hat{H}_{\vartheta, \varphi}^{min} = 2VK_1 \begin{pmatrix} 1 & 0 \\ 0 & 1 - h^2 \end{pmatrix} \quad (4.22)$$

$$\hat{H}_{\vartheta, \varphi}^{sad} = 2VK_1 \begin{pmatrix} h & 0 \\ 0 & h - 1 \end{pmatrix} \quad (4.23)$$

We calculate the determinants of the matrices and apply them to 4.3. This yields

$$\Omega_0 = \sqrt{\frac{1+h}{h}} \quad (4.24)$$

4.6 Multi-Spin Problem

4.6.1 Multi-Spin Spherical Hessian

Extending the formalism to tackle a system of an arbitrary number of spins, take a closer look at the structure of the $\hat{T}_{\{a_i\}}^N$ -operator. In the previous section we have seen, that when it acts on a scalar like the Gibb's Free Energy, $\hat{T}_{\{a_i\}}^N$ produces a matrix. This matrix is symmetric and all its entries are real, as long as there are only real entries in E .

For the Single Spin Problem this results in a 2×2 spherical Hessian, which we will refer to as \hat{H}_{11} . Using this notation, we can qualitatively line out a $N \times N$ -matrix for the N -Spin-Problem

$$\hat{H}_{\vartheta, \varphi} = \begin{pmatrix} \hat{H}_{11} & \hat{H}_{12} & \cdots & \hat{H}_{1N} \\ \hat{H}_{21} & \hat{H}_{22} & \cdots & \hat{H}_{2N} \\ \vdots & \vdots & \ddots & \vdots \\ \hat{H}_{N1} & \hat{H}_{N2} & \cdots & \hat{H}_{NN} \end{pmatrix} \quad (4.25)$$

where every entry represents a real 2×2 -matrix. Obviously the main diagonal consists exclusively of Single-Spin-like terms \hat{H}_{ii} . However, we must not be so naive as to not consider exchange interactions in those terms, because 4.18 teaches us that there is a contribution of \mathbf{H}_{eff} which - for Multi-Spin-Problems - contains the exchange field \mathbf{H}_{xch} .

Bearing this in mind, we take a look at the off-diagonal terms \hat{H}_{ij} with $i \neq j$. These matrices feature derivatives of E with respect to ϑ, φ on two different sites. The only way such a derivative is nonzero, is, if E depends on variables of two different sites. There is only one contribution to the Gibb's Free Energy that fulfills this requirement; the exchange energy. Since we take only next neighbor interactions into account, the exchange energy on the site i $E_{xch,i}$ is dependent on the two adjacent spins at sites $i \pm 1$ as well as the spin at the site i itself. Hence,

$$\hat{H}_{ij} = 0, \quad j = i \pm 2, i \pm 3, \dots \quad (4.26)$$

leaving only three diagonals in 4.25 nonzero. It is easily shown that

$$\hat{H}_{21} = \hat{H}_{12}^T \quad (4.27)$$

making $\hat{H}_{\vartheta, \varphi}$ a symmetric band matrix.

The 2×2 -elements \hat{H}_{ij} with $i \neq j$, have to be proportional to the exchange energy, all other contributions to E may not contribute, because they are canceled by the partial derivation. For the off-diagonal terms we arrive at the following expression.

$$\hat{H}_{ij} = -\frac{A}{a^2 J_s} \left[\begin{pmatrix} 1 & 0 & 0 \\ 0 & 1 & 0 \\ 0 & 0 & 1 \end{pmatrix} \left(\frac{\partial \mathbf{J}_i}{\partial (\vartheta, \varphi)_i} \right) \right] \cdot \left(\frac{\partial \mathbf{J}_j}{\partial (\vartheta, \varphi)_j} \right) \quad (4.28)$$

The partial derivatives with respect to (ϑ, φ) depends on which component of the 2×2 matrix is to be calculated. Simplifying the expression, we write the off-diagonal elements of $\hat{H}_{\vartheta, \varphi}$

$$\hat{H}_{ij} = -\frac{A}{a^2 J_s} \left(\begin{pmatrix} \left(\frac{\partial \mathbf{J}_i}{\partial \vartheta_i} \right) \cdot \left(\frac{\partial \mathbf{J}_j}{\partial \vartheta_j} \right) & \left(\frac{\partial \mathbf{J}_i}{\partial \vartheta_i} \right) \cdot \left(\frac{\partial \mathbf{J}_j}{\partial \varphi_j} \right) \\ \left(\frac{\partial \mathbf{J}_i}{\partial \varphi_i} \right) \cdot \left(\frac{\partial \mathbf{J}_j}{\partial \vartheta_j} \right) & \left(\frac{\partial \mathbf{J}_i}{\partial \varphi_i} \right) \cdot \left(\frac{\partial \mathbf{J}_j}{\partial \varphi_j} \right) \end{pmatrix} \right), \quad j = i \pm 1 \quad (4.29)$$

For a ferromagnetic state the exchange interaction keeps the spins parallel aligned to each other. Hence, we can assume that $\vartheta_i = \vartheta_j = \vartheta$ and $\varphi_i = \varphi_j = \varphi$. Inserting the polarization vector in spherical coordinates

$$\frac{1}{J_s} \mathbf{J} = \begin{pmatrix} \sin \vartheta \cos \varphi \\ \sin \vartheta \sin \varphi \\ \cos \vartheta \end{pmatrix} \quad (4.30)$$

and performing the derivation with respect to (ϑ, φ) , yields

$$\hat{H}_{ij} = -\frac{A J_s}{a^2} \begin{pmatrix} 1 & -\sin \vartheta \cos \vartheta \\ -\sin \vartheta \cos \vartheta & 1 \end{pmatrix}, \quad j = i \pm 1 \quad (4.31)$$

which for $\vartheta = \frac{\pi}{2}$ results in

$$\hat{H}_{ij} = -\frac{AJ_s}{a^2} \begin{pmatrix} 1 & 0 \\ 0 & 1 \end{pmatrix}, \quad j = i \pm 1 \quad (4.32)$$

We note that 4.31 is independent of φ . Since minimum and saddle-point configurations differ only in their φ -setting, not in their ϑ -setting, the off-diagonal terms of $\hat{H}_{\vartheta,\varphi}$ are identical for the respective Hessians.

Once more we observe the isotropic character of the exchange energy. Provided, that in both minimum and saddle-point configurations spins align parallel, the configurations themselves differ from one another in orientation. The off-diagonal terms of the respective Hessian feature only exchange contributions and due to the isotropy of the Heisenberg Hamiltonian remain oblivious to a change from minimum to saddle-point. The diagonal terms of the Hessian, however, must differ for different magnetization configurations, because they feature contributions of the anisotropy energy.

4.6.2 Explicit Calculations

Comparing different total system sizes with a variable number of spins, we get the plots in 4.1

We can see that Ω_0 is basically independent of the number of spins within a system, but is proportional to the total system size.

4.7 Eigenvectors and Eigenfunctions

For the calculation of Ω_0 we need the determinants of 4.25 at the minimum and saddlepoint of the Gibb's Free Energy. The determinant is the product of the eigenvalues λ_k that satisfy the equation

$$\hat{H}_{\vartheta,\varphi} \chi_k(\mathbf{r}) = \lambda_k \chi_k(\mathbf{r}) \quad (4.33)$$

$$\det \hat{H}_{\vartheta,\varphi} = \prod_k \lambda_k \quad (4.34)$$

4 Analytical Calculation of the Attempt Frequency

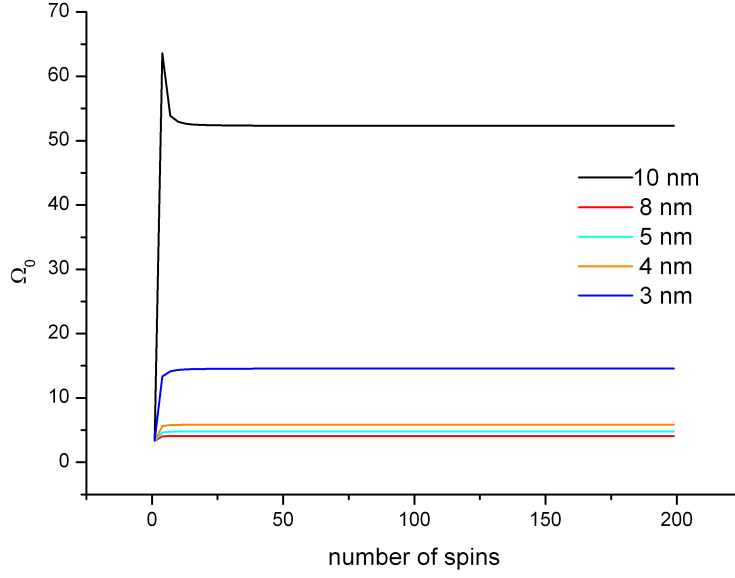


Figure 4.1: Ω_0 over number of spins for different total system sizes

with χ_k being the eigenvector or eigenfunction that is associated with λ_k . The set of all χ_k are a basis for the subspace of $\hat{H}_{\vartheta, \varphi}$. D'Aquino et al [Md09] formulated a spectral representation of Fourier modes, that allowed to write Gibb's Free Energy as

$$E_{dis} = \sum_k \frac{1}{2} \lambda_k a_k^2 - (\mathbf{h}_{ext}, \chi_k(\mathbf{r})) a_k \quad (4.35)$$

where $\chi_k(\mathbf{r})$ are the discretized magnetization Fourier modes, E_{dis} is the discretized Gibb's Free Energy, and (\mathbf{v}, \mathbf{w}) is the scalar product of $L^2(\Omega)$

$$(\mathbf{v}, \mathbf{w}) = \frac{1}{V} \int_{\Omega} \mathbf{v} \cdot \mathbf{w} dV \quad (4.36)$$

The spectral representation of spin-wave decomposition [Suh56] [GB01] is a good example of how magnetization can be expressed by means of Fourier plane-wave modes. The basic idea is to expand the magnetization through a Fourier series

$$\mathbf{u}(\mathbf{r}, t) = \sum_{k=1}^{\infty} a_k(t) \chi_k(\mathbf{r}) \quad (4.37)$$

with

$$a_k(t) = (\mathbf{u}(\mathbf{r}, t), \chi_k(\mathbf{r})) \quad (4.38)$$

Modes of lower k correspond to a lower energy contribution, making χ_0 the ground state mode, which we expect to show all spins aligned parallel in minimum direction. Higher modes represent excitations and refer to higher energy contributions.

The representation of the eigenfunctions $\chi_k(\mathbf{r})$ is not well defined, since the used norm is relevant. Consider a unit eigenvector

$$\chi_e = \begin{pmatrix} \vartheta_e \\ \varphi_e \end{pmatrix} \quad (4.39)$$

giving a solution of equation 4.33. Every new set

$$\chi' = \begin{pmatrix} \vartheta'_e \\ \varphi'_e \end{pmatrix} = s \begin{pmatrix} \vartheta_e \\ \varphi_e \end{pmatrix} \quad s \in \mathbb{R} \quad (4.40)$$

would provide an equal solution. Within a coordinate system of axis (ϑ, φ) , such a transformation would keep the orientation of the vector intact and for $s \in (-\infty, \infty)$ defines a straight line 4.2

However, if we map this function on the x, y, z -space using the usual transformations

$$\begin{pmatrix} \chi_x \\ \chi_y \\ \chi_z \end{pmatrix} = \begin{pmatrix} \sin(s\vartheta_e) \cos(s\varphi_e) \\ \sin(s\vartheta_e) \sin(s\varphi_e) \\ \cos(s\vartheta_e) \end{pmatrix} \quad (4.41)$$

the straight line becomes a rather complex curve on the surface of a sphere 4.3

This means that orientations of the eigenvector modes is depending on the norm s . As long as this is kept in mind and the same norm (e.g. $s = 1$) is used for all representations of χ_k , no qualitative information is lost.

A $2N \times 2N$ -matrix has $2N$ eigenvectors, hence $k = 0, 1, 2, \dots, 2N - 1$. Each eigenvector has $2N$

4 Analytical Calculation of the Attempt Frequency

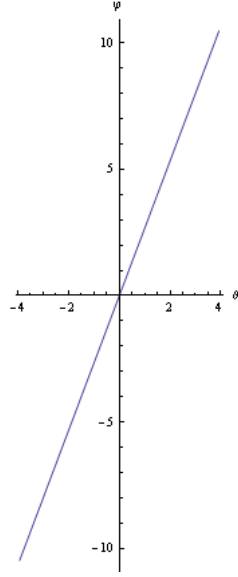


Figure 4.2: Eigenvector within (ϑ, φ) -coordinate system

components. The components represent (ϑ, φ) -coordinates for all spins.

$$\chi = \begin{pmatrix} \vartheta_1 \\ \varphi_1 \\ \vartheta_2 \\ \varphi_2 \\ \vdots \\ \vartheta_N \\ \varphi_N \end{pmatrix} \quad (4.42)$$

These eigenvectors are transformed into a cartesian representation and plotted. For lower excitations of a 30-spin-system we get rather beautiful wave-like eigenfunctions $\chi_k(\mathbf{r})$ like in [4.4 - 4.7](#)

For higher excitations this representation is no longer gentle to the eye and we choose at glyph-representation, where colors correspond to J_z -values of the local polarization vector.

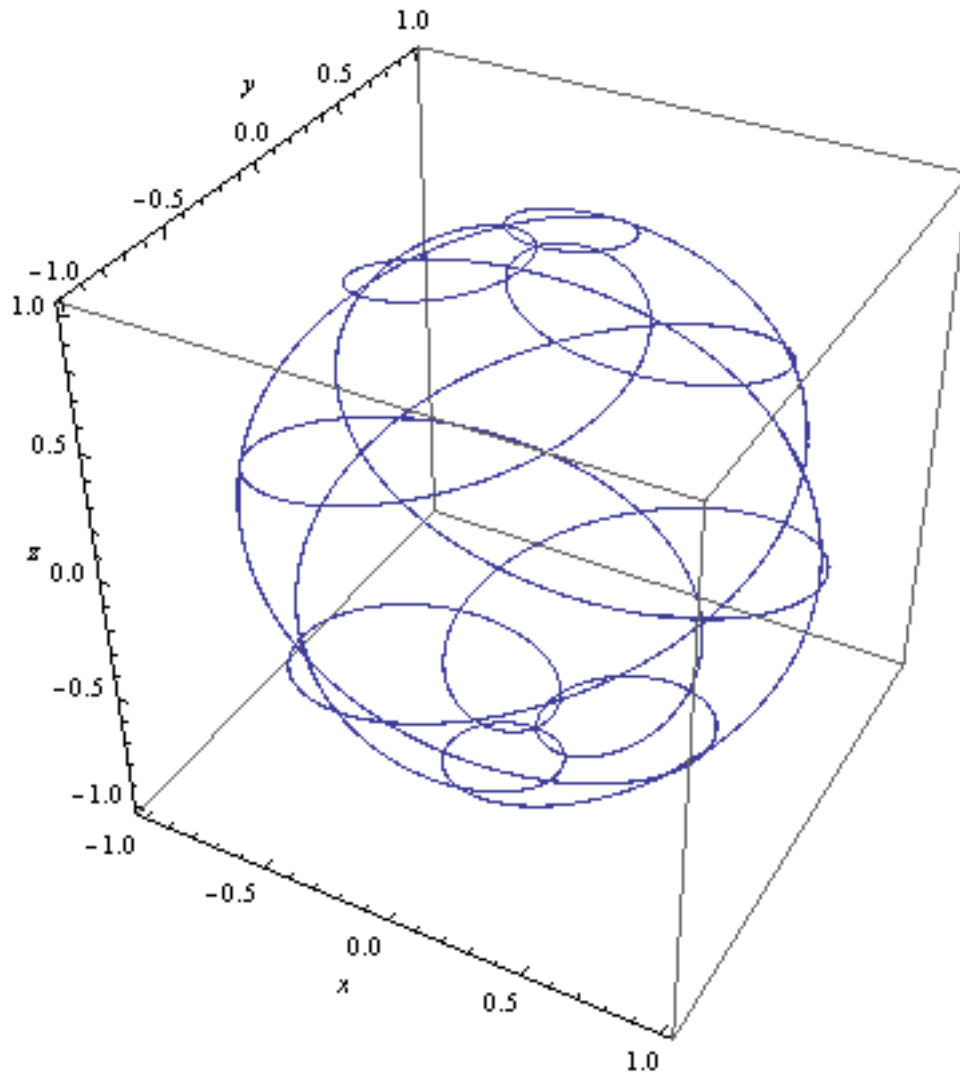


Figure 4.3: Eigenvector within (x, y, z) -coordinate system

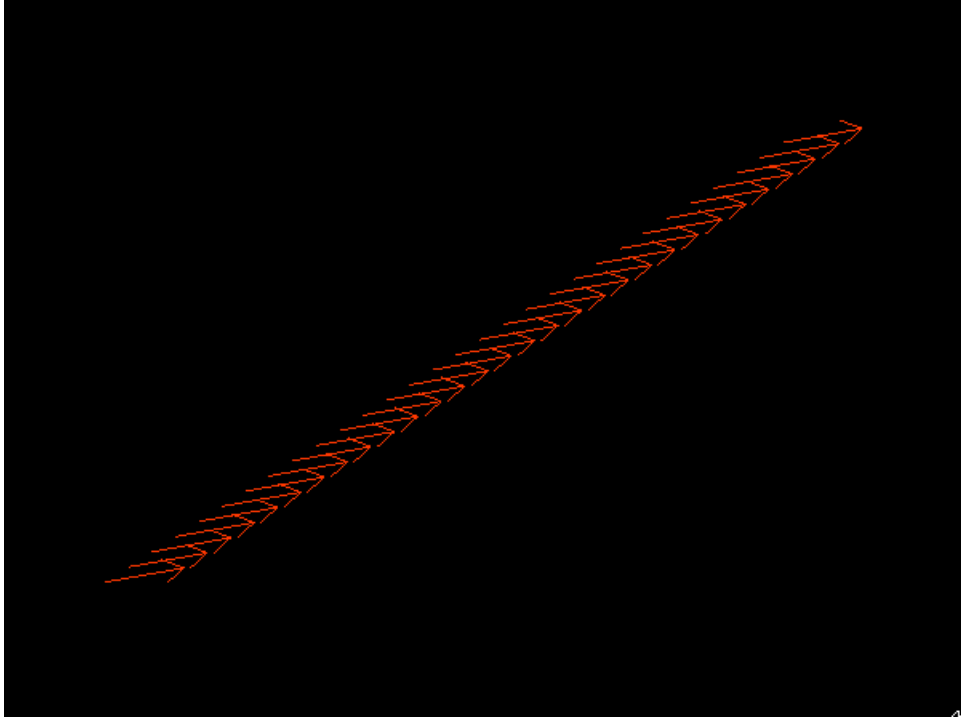


Figure 4.4: *mode = 0, groundstate*

4.8 Eigenvalue Analysis

The ordering of the eigenvalues by magnitude allows us to take a look at the ratios $\frac{\lambda_k^{min}}{\lambda_k^{sad}}$. Numerical calculations of 3nm system consisting of 30 (figure 4.13) respectively 300 (figure 4.14) spins are shown here. The numerical solutions were fitted by an exponential function and a critical exponent was found.

We observe that the fitting function quite rapidly converges to zero, and deduce that after a critical k -value all fractures $\frac{\lambda_k^{min}}{\lambda_k^{sad}}$ equal one, and therefore do no longer contribute to the attempt frequency. This gives rise to the idea that the complexity could be drastically reduced, if a formalism was derived, that determines how many k -values need to be taken into account for a sufficient numerical solution. The formalism shows no dependency on the number of spins.

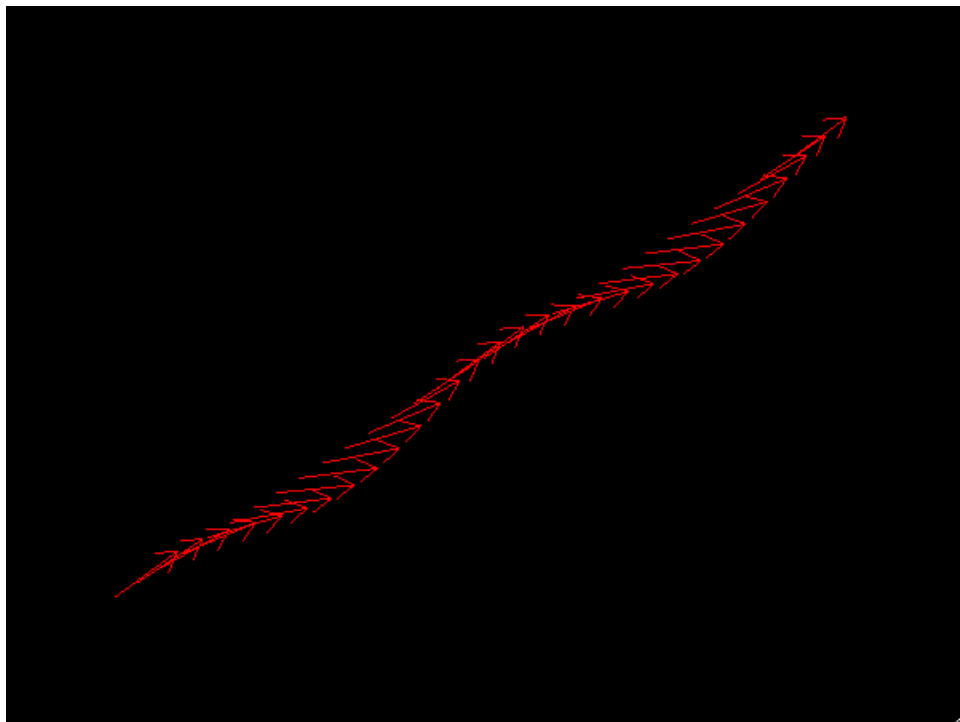


Figure 4.5: $mode = 8$

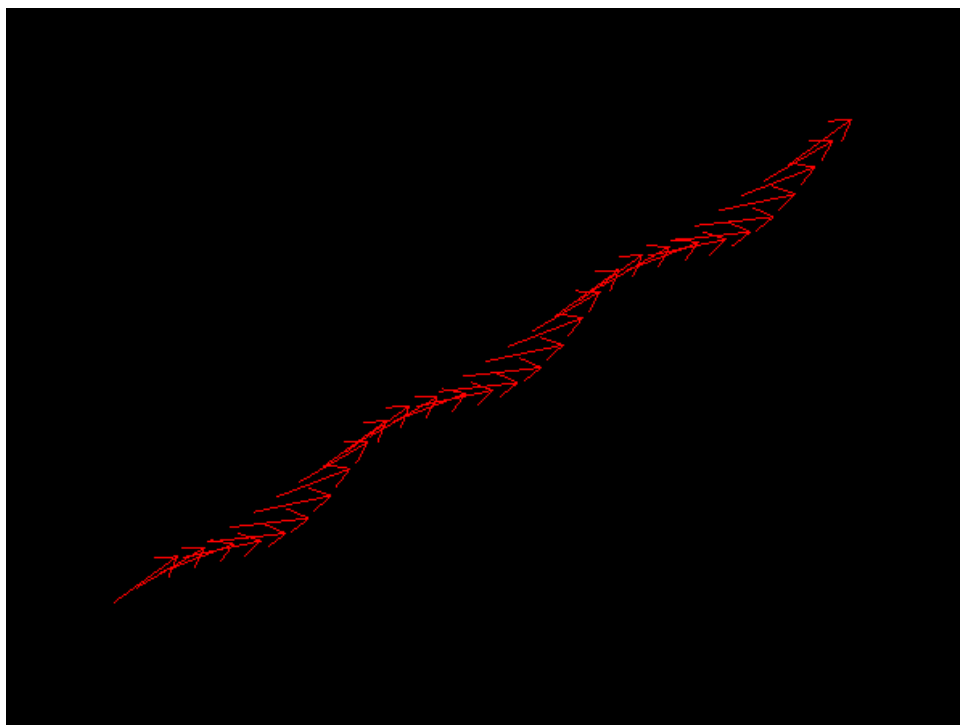


Figure 4.6: $mode = 12$

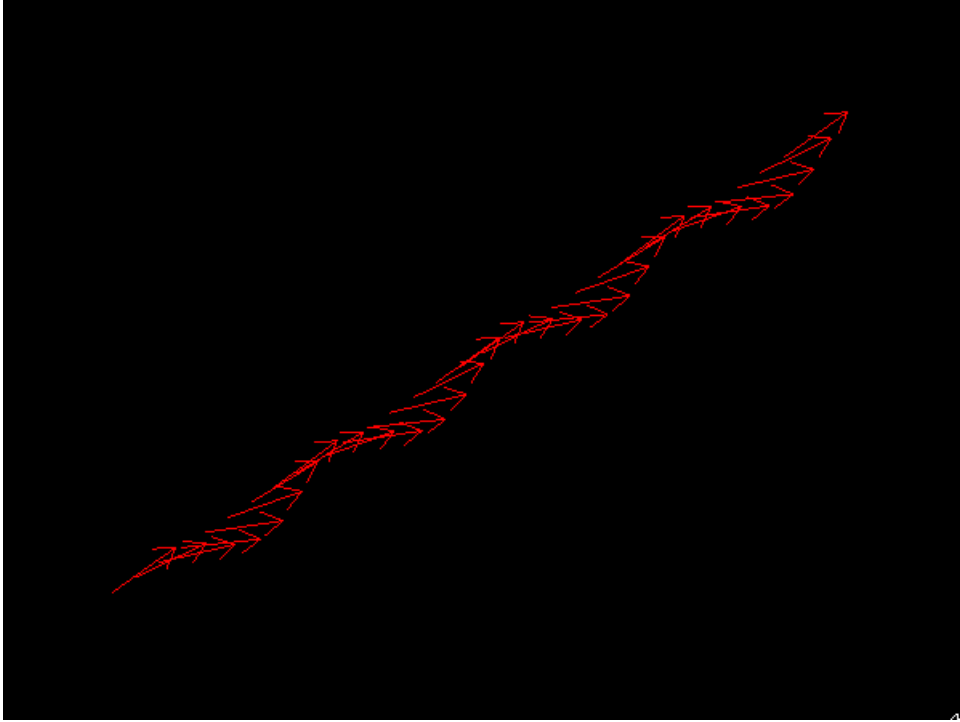


Figure 4.7: $mode = 16$

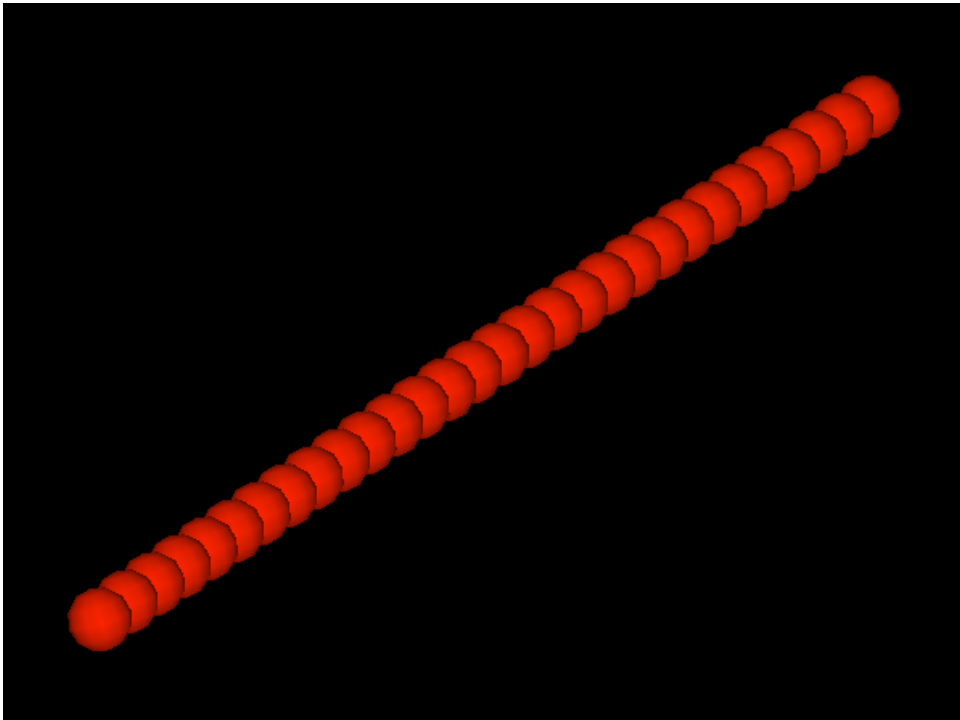


Figure 4.8: $mode = 0, groundstate$

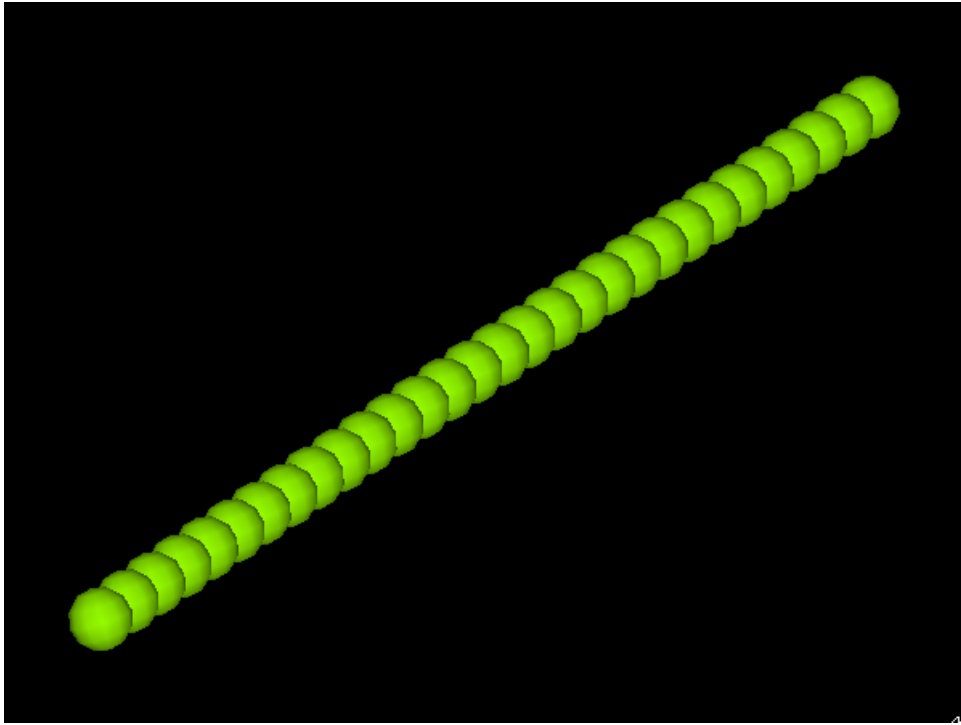


Figure 4.9: $mode = 1$, $firstexcitation$

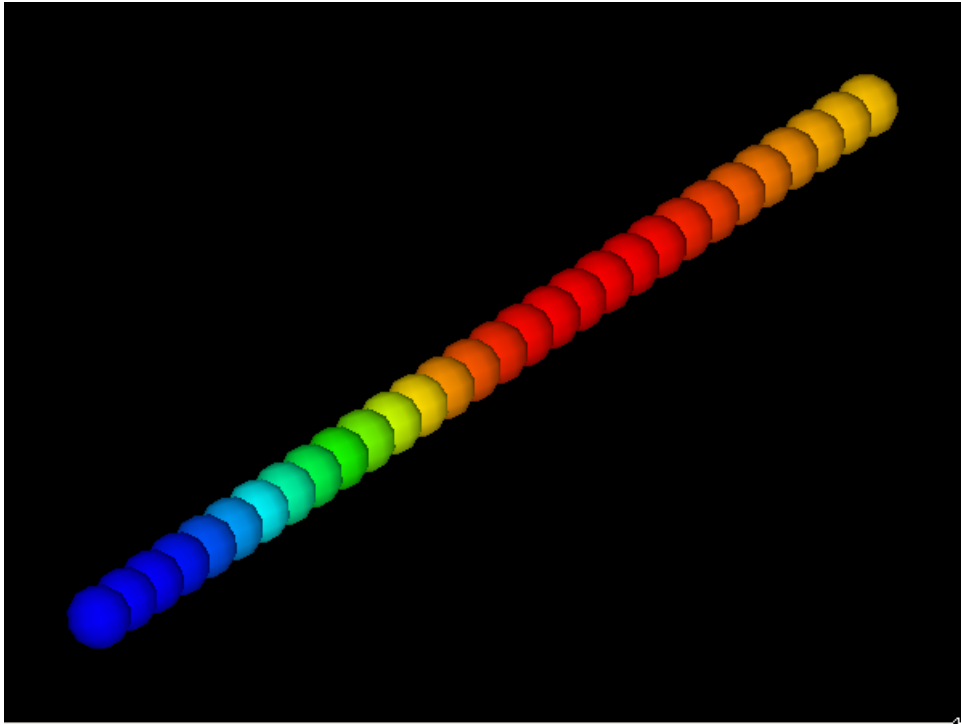


Figure 4.10: $mode = 2$

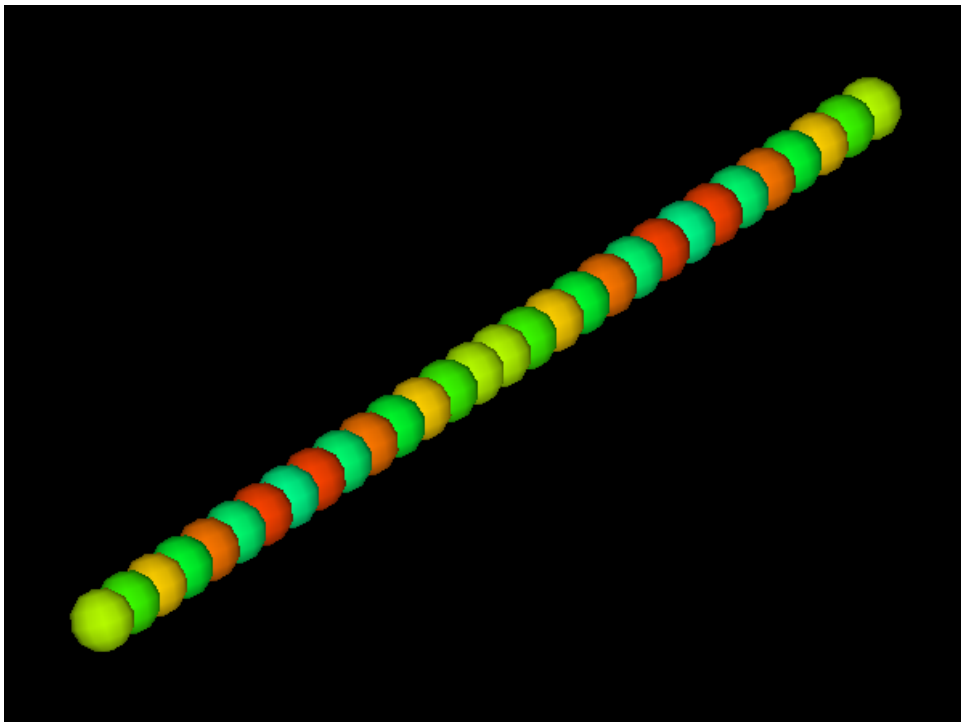


Figure 4.11: $mode = 33$

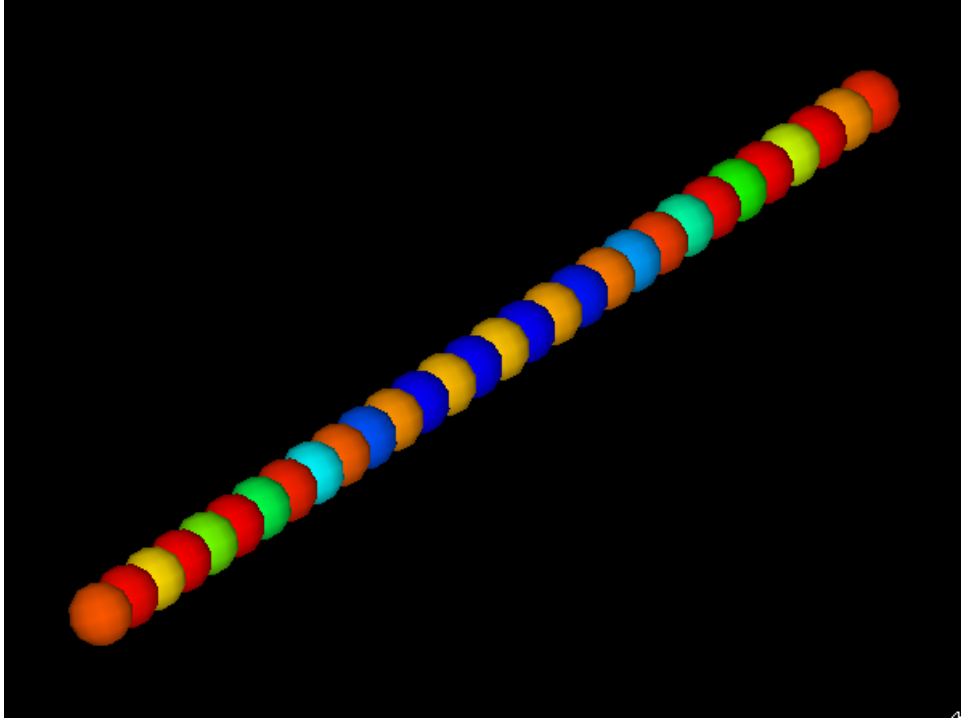


Figure 4.12: $mode = 58$

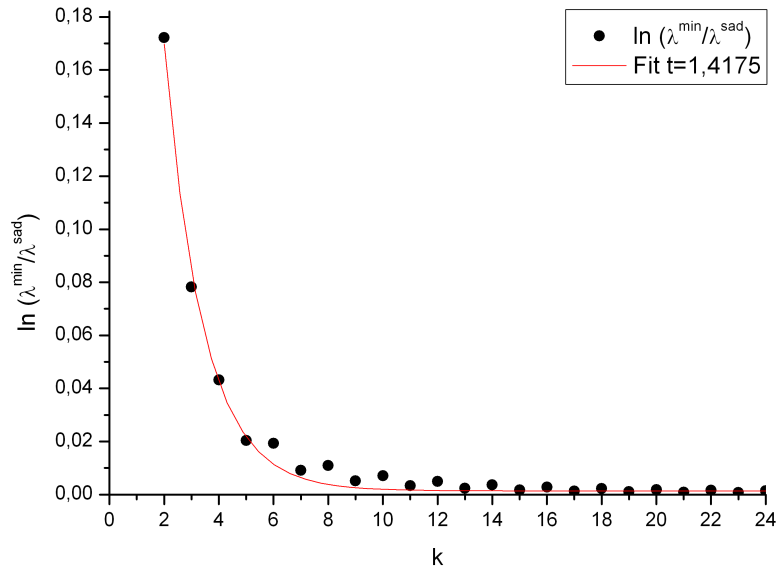


Figure 4.13: $\ln \frac{\lambda_k^{\min}}{\lambda_k^{\text{sad}}}$ over k for 3nm system size and 30 spins; fit with $a \exp\left(-\frac{k}{t}\right)$

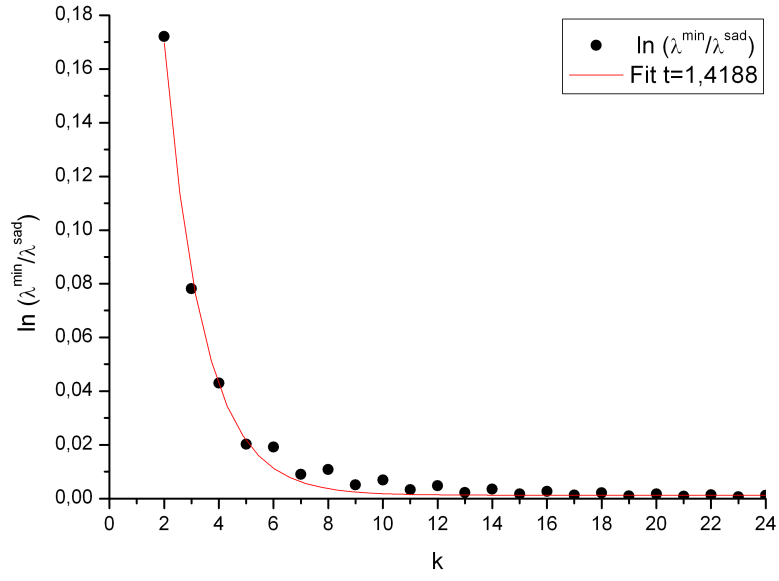


Figure 4.14: $\ln \frac{\lambda_k^{\min}}{\lambda_k^{\text{sad}}}$ over k for 3nm system size and 300 spins; fit with $a \exp\left(-\frac{k}{t}\right)$

5 Conclusion and Outlook

The analysis of single domain dynamics predicts uniform movement for spins in a magnetic chain. Regardless of system size and number of spins, the exchange integral accounts for ferromagnetic (parallel) or anti-ferromagnetic (antiparallel) alignment. Magnetization alteration by means of an externally applied magnetic field shows a dependency of the coercivity field on the anisotropy constant, resulting in the fact that with increased stability of state there comes a higher strain for magnetization switching. The statistical factor of the attempt frequency is independent of the number of spins within the micromagnetic system, but simulations predict a dependency on the total system size. A closer look at the eigenvalues shows that for an accurate calculation of the statistical factor, it suffices to take only a few eigenvalues into account, reducing computing time and complexity of the problem. For future considerations, this routine may also be extended to tackle 3-dimensional systems of different material properties (e.g. different anisotropies, nearest-neighbor-distance, . . . etc).

6 Bibliography

- [Aha96] A. Aharoni. Introduction to the theory of ferromagnetism, 1996.
- [Bra94] H.-B. Braun. Kramer's rate theory, broken symmetries, and magnetization reversal. J. Appl. Phys. **76**,10, 1994.
- [Bro63a] W.F. Brown. Phys. Rev. **130**, 1677, 1963.
- [Bro63b] W.F. Brown. Micromagnetics, 1963.
- [DB99] J.J. Gray D.A. Brannan, M.F. Esplen. Geometry. 328, 1999.
- [EPCF08] F. Garcia-Sanchez E. Paz and O. Chubykalo-Fesenko. Physica B **402**, 330, 2008.
- [GB01] C. Serpico G. Bertotti, I. Mayergoyz. Phys. Rev. Lett. **87**, 2001.
- [GB06] I. Mayergoyz G. Bertotti. The science of hysteresis, 2006.
- [Kra40] H.A. Kramers. Brownian motion in a field of force and the diffusion model of chemical reactions. Physica **7**, 284, 1940.
- [Lan67] J. S. Langer. Ann. Phys. **41**, 108, 1967.
- [Md09] G. Bertotti T. Schrefl I. Mayergoyz M. d'Aquino, C. Serpico. Spectral micromagnetic analysis of switching processes. J. Appl. Phys. **105**, 2009.
- [N49] L. Néel. Ann. Géophys. **5**, 99, 1949.
- [RDF02] D. Suess W. Scholz H. Forster [4] R. Dittrich, T. Schrefl and J. Fidler. J. Magn Mag. Mat. **250**, 12, 2002.
- [Sch06] W. Scholz. Master's thesis, Vienna University of Technology, 2006.
- [Sch09] J. Schratzberger. Master's thesis, Vienna University of Technology, 2009.
- [Sue99] D. Suess. Master's thesis, Vienna University of Technology, 1999.
- [Suh56] H. Suhl. Proc. IRE **44**, 1270, 1956.